Chair of Petroleum and Geothermal Energy Recovery

Master's Thesis

Business opportunities to extend Oil Well Life Recovering Geothermal Energy in the Vienna Basin

David Timpl, BSc

April 2022

MONTANUNIVERSITÄT LEOBEN
www.unileoben.ac.at

EIDESSTATTLICHE ERKLÄRUNG

Ich erkläre an Eides statt, dass ich diese Arbeit selbständig verfasst, andere als die angegebenen Quellen und Hilfsmittel nicht benutzt, und mich auch sonst keiner unerlaubten Hilfsmittel bedient habe.

Ich erkläre, dass ich die Richtlinien des Senats der Montanuniversität Leoben zu "Gute wissenschaftliche Praxis" gelesen, verstanden und befolgt habe.

Weiters erkläre ich, dass die elektronische und gedruckte Version der eingereichten wissenschaftlichen Abschlussarbeit formal und inhaltlich identisch sind.

Datum 21.04.2022

Unterschrift Verfasser/in
David Timpl

MONTANUNIVERSITÄT LEOBEN
www.unileoben.ac.at

AFFIDAVIT

I declare on oath that I wrote this thesis independently, did not use other than the specified sources and aids, and did not otherwise use any unauthorized aids.

I declare that I have read, understood, and complied with the guidelines of the senate of the Montanuniversität Leoben for "Good Scientific Practice".

Furthermore, I declare that the electronic and printed version of the submitted thesis are identical, both, formally and with regard to content.

Date 21.04.2022

Signature Author
David Timpl

Danksagung

Mein Dank gilt Lehrstuhlleiter Univ.-Prof. Dipl.-Ing. Dr.mont. Herbert Hofstätter für die Bereitstellung dieser Arbeit.

Besonders danke ich Dipl.-Ing. Dr. Rudolf Fruhwirth für die sehr gute Betreuung und für die Bereitstellung der Software zur Simulation des Bohrlochwärmetauschers. Er hat mit hilfreichen Anregungen und konstruktiver Kritik geholfen, dafür möchte ich mich herzlichst bedanken.

Weiters bedanke ich mich bei Dipl.-Ing. Robert Maier, für die Betreuung von Seiten der OMV, und dafür, dass er immer ein offenes Ohr für mich hatte.

Ein großer Dank gilt meinen Eltern, die mir mein Studium ermöglicht haben.

Kurzfassung

Am Ende ihrer Lebensspanne werden Öl- und Gasbohrlöcher normalerweise verfüllt und renaturiert. Damit wird jede Möglichkeit, diese Bohrlöcher noch einem sinnvollen Zweck zuzuführen, zunichte gemacht. Eine Chance, das zu verhindern ist die Bohrlöcher neu zu komplettieren und zur Gewinnung geothermaler Energie zu nutzen. Die Umwandlung von nicht mehr gewinnbringenden Öl und Gassonden ist eine gute Geschäftsmöglichkeit, wenn man bedenkt, dass die Energie nicht nur nachhaltig gewinnbar, sondern auch CO_2 - frei ist.

In dieser Arbeit werden potenzielle Anwendungsmöglichkeiten, für die aus Bohrlöchern im Wiener Becken gewinnbare Energie untersucht. Dazu wurde das Verhalten eines Gegenstrom Bohrlochwärmetauschers, unter verschiedenen Einflusstemperaturen, Ausflusstemperaturen, Durchflussraten, Konduktivitäten und Teufen simuliert und in Diagrammen visualisiert. Mit den Ergebnissen dieser Simulationen wurden unterschiedliche Anwendungsmöglichkeiten auf ihre Realisierbarkeit in Bezug auf Temperatur- und Energiebedarf abgeschätzt, sowie die Möglichkeit geschaffen, das auch für andere Applikationen zu tun. Eine zweite Möglichkeit, Bohrlöcher einem neuen Zweck zuzuführen und dadurch ihre Lebenszeit zu verlängern, besteht darin, sie als Zugang zur ausgebeuteten Lagerstätte zu verwenden und diese als thermischen Speicher zu verwenden. Diese Möglichkeit wird anhand einer Literaturrecherche über den geothermalen Tiefenspeicher in Neubrandenburg diskutiert. Es werden seine Effizienz und Verlässlichkeit sowie auch die dortigen Probleme aufgezeigt.

Abstract

Oil and gas wells at the end of their life span, are generally plugged, the landscape is restored and abandoned. Thus, all further possibilities to convert the wells for alternative use is lost. One possibility to re- or further use the wells is to re-complete and use the wells for geothermal energy production. The conversion of not economic oil and gas wells to produce renewable energy seems to be a valid business opportunity considering that not only geothermal energy is produced but also a positive impact on CO_2 emission reduction is given.

The thesis studies the potential geothermal energy production from typical oil and gas wells in the Vienna basin, its use and applications. The energy, which can be produced by a borehole heat exchanger in reverse circulation was calculated, for wells at different depth, different thermal rock conductivities, various circulating flowrates, and several out- and inflow temperatures. The results are presented in plots within this thesis. The diagrams allow a quick evaluation of the energy potential the individual well can produce and estimate the opportunity level of the anticipated business application. Applications for geothermal energy produced from oil and gas wells at the end of their lifespan were investigated. Common business applications were chosen to explain the use of the calculated general information and demonstrate its value at a first glance to understand the business opportunity. Finally, because not only the well itself, but also the adjacent reservoir can be used as thermal storage, a literature review on the Neubrandenburg aquifer thermal energy storage was examined. Its efficiency and reliability as well as the problems of this project are discussed.

Table of Content

Page

1 Introduction

Drilling costs are usually a major factor in geothermal energy production. Especially when compared with the possible revenues coming from geothermal applications in areas with limited geothermal gradients e.g. 3°C in the Vienna basin. With regards to the environmental impact caused by CO_2 emissions, geothermal energy production is predestined to be used as an environment-friendly green energy source. Thus, the potential of existing oil and gas wells, which are not economically produced anymore, should be evaluated with respect to geothermal energy production.

Technically geothermal energy can be produced from converted oil and gas wells. Two different production techniques can be distinguished. One is the energy extraction from the cased borehole only, and the other one is the usage of the adjacent reservoir. In the following, ideas for both cases will be presented. Because of its simplicity and therefore wider range of application the production of geothermal energy using closed loop heat exchangers is prioritized and investigated more in detail. Although the main disadvantage of a closed loop heat exchangers is the relative low energy exchange capacity, the systems bring advantages of being safe, easy to be operated and cost efficient. The major drawback is the low efficiency, and thus low temperature and energy production levels.

The cornerstone of this thesis are simulations of the performance of a borehole heat exchanger under different operating conditions and formations surrounding it. The simulation results are summarized in a compendium of graphs which provide the engineer with the information necessary to evaluate the energy potentially produced from an existing well. Subsequently the engineer has the possibility to classify the well quality for different business applications. This easy and quickly gained information can be explicitly translated to business unit sizes, based on the power and temperature requirements of applications such as greenhouses, aquacultures, or bio-gas production facilities.

Further usage for oil and gas wells that have reached the end of their lifespan is to utilize the reservoir they are connected to. Aquifer thermal energy storage is a promising technology. It was experimented in Neubrandenburg from 2005 to 2019 and was investigated in terms of its origin, development, and performance.

2 Fundamentals

“Geothermal energy is energy contained within the high temperature mass of the Earth’s crust, mantle, and core. Since the Earth’s interior is much hotter than its surface, energy flows continuously from the deep, hot interior up to the surface. This is the so-called terrestrial heat-flow. The temperature of the Earth’s crust increases with depth in accordance with Fourier’s law of heat conduction. Thus, the energy content of a unit of mass also increases with depth” (Toth, 2016). For deeper geothermal systems (>300m) there are several ways to extract this energy, depending on the type of Geothermal system present. In a hydrothermal system energy is produced from an aquifer using a geothermal doublet, where one well is used for injection and the other well for production. Geothermal energy production is also possible by using downhole heat exchangers. Downhole heat exchangers can be engineered within the subsurface by fracturing the formation and creating a flow path for the injected fluid. This is called an Enhanced Geothermal System (EGS). Other than that, closed loop heat exchangers can be used (Langbauer, 2020). Such are coaxial and U-tube heat exchangers. However, for the purpose of extending oil and gas well life in the Vienna basin the use of closed loop heat exchangers for heat extraction is most beneficial, because of the clear separation from the reservoir and thus safe, steady, and carefree operation.

2.1 Fundamentals of closed loop borehole heat exchangers

Two different designs are available, the U-tube heat exchanger and the coaxial heat exchanger. For the use as a borehole heat exchanger, the coaxial heat exchanger is used, as its performance is superior. The bigger the area at which heat is exchanged, the better its performance. Since the coaxial type utilizes the whole wellbore, it is superior to the U-tube heat exchangers which can only utilize it partly. There are other designs including demi-types of the U-Tube and the Coaxial heat exchanger, but they very rarely have any practical use (Śliwa et al., 2017).

Coaxial heat exchangers can be run in direct circulation meaning injection through the tubing and production from the annulus or in reverse circulation meaning injection through the annulus and production from the tubing. In Figure 1 a Coaxial borehole heat exchanger in reverse circulation with a vacuum insulated tubing is shown. Different parts shown in figure 1 are: “**1**: heat recipient (with/without heat pump), **2**: casing, **3**: outer pipe of double-layered coaxial column, 4: annular between inner and outer double column, **5**: inner pipe of double coaxial column, **6**: heat carrier in inner column, **7**: heat carrier in annular between inner column and casing, **8**: cement plug and/or packer” (Śliwa et al., 2017).

Overall heat transfer is defined by the structure of the heat exchanger. Three heat exchange mechanisms dependent on each other must be considered. Radial heat conduction from the formation supplies the system with thermal energy. Subsequent the heat is transferred into the down-flowing fluid, which reaches its highest temperature bottomhole. The third heat transfer mechanisms occurs when the fluid is flowing back upwards, where heat is transferred back into the annulus. Considering this, it becomes evident, that an insulated tubing, restricting the

heat transfer back into the annulus improves the performance. The base-case is a single steel coaxial inner column, which is the cheapest, but less efficient option in terms of insulation. Better is a double steel coaxial inner column with insulation fluid which could be nitrogen or air. Coated pipes are similar to the double steel coaxial tubing. They have a layer of insulating material like polyurethane applied to their surfaces. Most beneficial are vacuum insulated tubings. They decrease the heat flow depending on the grade of vacuum applied significantly (Śliwa et al., 2017). This is because conductive and convective heat transfer is suppressed almost completely.

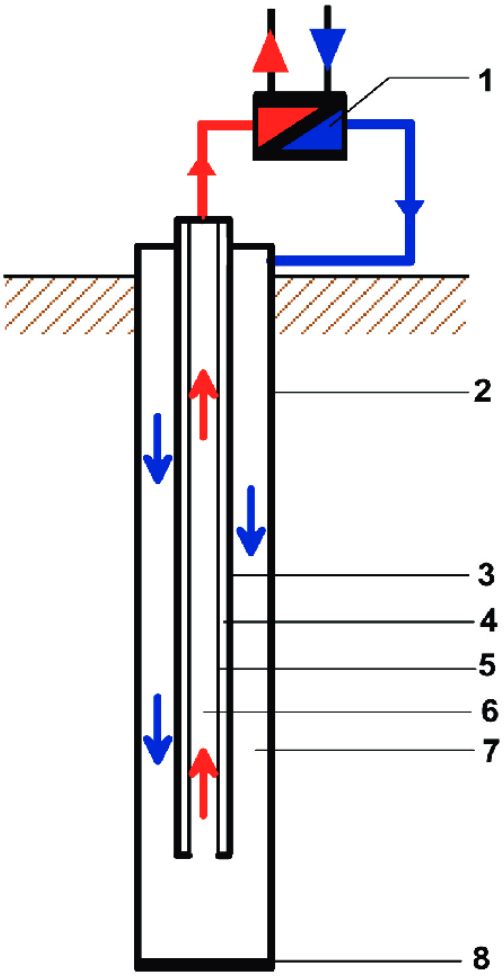

Figure 1: Borehole heat exchanger in reverse circulation[1]

2.2 Fundamentals of heat transfer inside the borehole heat exchanger

Heat transfer in the formation and the borehole heat exchanger governs the geothermal potential of wells. And thus, their usefulness for business applications to extend oil and gas well life in the Vienna basin.

[1] Śliwa, T., Kruszewski, M., Sapińska-Śliwa, A. and Assadi, M. (2017) 'The application of Vacuum Insulated Tubing in Deep Borehole Heat Exchangers', *AGH Drilling, Oil, Gas*, vol.34, no.2, p.602

Engineers when using borehole heat exchangers require both, a good understanding of the heat transfer inside the system. And the ability to calculate the geothermal power produced, the outflow temperature and the pumping power required for sustaining circulation. Both, understanding and calculating heat transfer is best done by separating the system into two parts heat transfer through the formation and heat transfer inside the formation.

Temperature difference is the driving factor for heat transport as it represents the potential for heat to be transported. Depending on the mode of transportation and temperature differences heat flows at a specific rate, in the direction of decreasing temperature. In a borehole heat exchanger, the temperature difference is the one between the borehole wall and the fluid in the annulus. Conduction, convection, and radiation are the modes of heat transfer to be considered. Conductive heat transfer is described by Fouriers Law and is the transfer mechanism occurring between all particles. Fouriers Law is shown in equation 1. In solid materials like in the piping and the cement heat flow is purely conductive. Convective heat transfer happens between a surface and a fluid, it is described by Newton´s Law of cooling shown in equation 2. Convective heat transport can be free and forced and is responsible for the heat transport between the piping and the flowing fluid in the borehole heat exchanger. It combines the effects a fluid in motion has on heat transport with conductive heat flux. Stefan Boltzmann´s law of radiation is important for describing the heat transfer inside a vacuum isolated tubing. Radiation is the only heat transfer mode present. It is shown in equation 3 (Cengel, 2011).

$$\dot{Q} = \frac{kA}{L}(T_1 - T_2) \qquad \text{(Eq. 1)}$$

$$\dot{Q} = hA(T_1 - T_2) \qquad \text{(Eq. 2)}$$

$$\dot{Q} = \epsilon\sigma A T_s^4 \qquad \text{(Eq. 3)}$$

In the formulas $\dot{Q}$ is the rate of heat transfer in Watts, k is the conductivity in [W/mK] of the respective material and A is the Area on which the heat transfer happens. Further, h is the heat transfer coefficient in [W/m^{2}K], ϵ is the unitless emissivity of the surface and σ is the Stefan Bolzmann constant in [W/m^{2}K^4].

Radiative heat transfer is the weakest mode of transportation appearing in a borehole heat exchanger. Overall heat conductivity for a vacuum insulated tubing is between 0,06 and 0,0008 W/mK which is very small when compared to steel with its 50 W/mK or even fiber glass with a conductivity of 0,361 W/mK (Śliwa et al., 2017).

Linking the modes of heat transfer to describe the heat flux from the borehole wall to the annulus is best done by introducing the concept of thermal resistivity as shown in equation 4. Utilizing it allows the overall heat transfer to be described easier. As heat is transported through the borehole from the higher temperature outside to the lower temperature in the annulus it must overcome different thermal resistances. This approach is valid for steady state heat flux.

$$\dot{Q} = R^{-1}\,\Delta T \qquad \text{(Eq. 4)}$$

Comparing equation 4 with equations 1 and 2 resistivity for conductive and convective heat transport takes the form as shown in equation 5 and 6.

$$R_{conduction} = \frac{L}{kA} \qquad \text{(Eq. 5)}$$

$$R_{convection} = \frac{1}{hA} \qquad \text{(Eq. 6)}$$

Key for applying the concept of thermal resistivity for conductive heat flow is the conductivity k. Conductivity is dependent on temperature and material. The higher the thermal conductivity is the easier heat flows (Cengel, 2011).

Convective resistivities are harder to assess since they do not depend only on the material and the temperature of the surface but also on flow properties of the fluid. Generally speaking, fluid movement increases heat flux since convective transport without fluid movement would just be conductive transport. For a precise description of this fact a dimensionless number is needed, the Nusselt number. It describes the ratio of convection to pure conductive heat transfer on a surface (Cengel, 2011).

$$Nu = \frac{convection}{pure\ conduction} = \frac{hL}{k_f} \qquad \text{(Eq. 7)}$$

Where L is the characteristic length, h is the heat transfer coefficient and k_f is the conductivity of the fluid. Calculating the heat transfer coefficient and thus make it possible to determine the convective resistivity is possible when the other variables in equation 7 are known. Determining the Nusselt number is done differently depending on the mechanism causing the fluid flow. Forced convection occurs when the flow is caused by an external source. Natural convection occurs when flow is induced by buoyancy differences which are caused by temperature differences. The Nusselt number can be correlated with the Reynolds number and the Prandtl number when convection is forced. It can be correlated with the Grashof Number and the Prandtl Number if natural convection is dominant (Fruhwirth, 2020/21). The Grashof, Prandtl and Reynolds Number are used for describing flow properties. Description of the flow properties is also important for calculating the power demand to pump the fluid through the borehole heat exchanger. Therefore Grashof, Reynolds and Prandtl dimensionless numbers are described briefly in equations 8 to 10. For the Reynolds number ρ is the density of the fluid, d is the diameter of the pipe, v is the flow velocity and η is the dynamic visosity.

$$Gr = \frac{Buoyancy\ force}{Viscous\ force} \qquad \text{(Eq. 8)}$$

$$Re = \frac{Inertia\ Forces}{Viscous\ Forces} = \frac{\rho v d}{\eta} \qquad \text{(Eq. 9)}$$

$$Pr = \frac{Viscous\ diffusion\ rate}{Thermal\ diffusion\ rate} \qquad \text{(Eq. 10)}$$

A Nusselt number close to one is characteristic for sluggish flow or laminar flow. Convection and conduction appear at the same order of magnitude. Larger Nusselt numbers (100-1000) typically appear when turbulent flow is present (Fazeli, 2020).

Addressing all factors influencing the resistivity inside the borehole and calculating them is only possible by using a simulator.

3 Simulation of heat transfer in borehole heat exchangers

The goal of the simulation was determining the power output, the outflow temperature level, and the hydraulic power demand of a borehole heat exchanger under different operating conditions. The following chapter describes the principles of the simulation software used for this purpose called WellUse. The simulated cases as well as the visualization of the results are elaborated. Water is the medium chosen to be used for simulations, because it has a high heat capacity is easy manageable and inexpensive as well as almost incompressible. The energy output and the outflow temperature depend on the flowrate, the inflow temperature, and the conductivity of the surrounding formation. Also, efforts to keep the visualization of the data comprehensible and understandable is discussed in this chapter.

3.1 Simulation software

The program consists of two parts, the calculation of the heat transfer in the formation with the earth model and the calculation of the heat transfer inside the borehole with the borehole model. WellUse can also calculate the hydraulics of the heat exchanger. The program subdivides the borehole into multiple elementary sections along its axis for which deterministic solutions of the conservation equations for mass, energy and momentum are available. WellUse determines friction and hydrostatic pressure losses in the annulus and the tubing. The description of the fluid flow although, is simplified by the assumption of an incompressible fluid circulating through the piping (Fruhwirth and Hofstätter, 2016, p. 490).

3.1.1 Heat transfer in the earth model

Calculation of the thermal properties in the Formation and the Heat exchanger are, as mentioned, done separately. The two subsections are coupled via the borehole-wall temperature and the constant heat flow per section length between the borehole and the formation. By its nature the heat transfer in the formation is transient. Calculating the heat transfer inside the formation without extensive computing time, is done by utilizing the deterministic Line Source model developed by Lord Kelvin. The line source model allows the temperature of the earth to be modelled as a function of time, distance from the source and the amount of heat removed from the formation (Fruhwirth and Hofstätter, 2016, p. 491).

3.1.2 Heat transfer inside the well

When looking at the heat transfer in the well, two different transfers must be considered. Heat transfer from the formation through the cement and the casing into the annulus and the heat transfer from the tubing into the annulus. While the heat transfer from the casing in the annulus increases the temperature of the down-flowing fluid, the heat transition from the tubing into the annulus reduces the temperature of the fluid travelling to the surface.

Minimizing this effect geothermal installations generally use, as mentioned before, insulated tubings. For this thesis the tubing is assumed to be perfectly insulated in order to provide a

base case and because of the possibility to use vacuum insulated tubings is rather close to the ideally isolated one.

All three different heat transfer mechanisms act within the heat exchanger if the tubing is not considered to be perfectly isolated. Forced and free convection appear in the fluid. Radiation in the vacuum isolated tubing wall (if used) and conduction appears in the fluid and the piping. For applying the different heat transfer mechanisms, the thermodynamic resistivities are calculated via correlations based on the Nusselt Number. Namely the Petukhov-Popov and Gnielinski for forced convection and the model from Dropkin and Somerscales for natural convection (Fruhwirth and Hofstätter, 2016, p. 491).

The Petukhov-Popov model is a correlation using the Reynolds and the Prandtl number and is valid for a broad range of Prandtl numbers and is good suited for more turbulent flow, since it is valid for Reynolds number values from 10^4 to $5x10^4$ (Lorenz et al., 1982) The Gnielinski equation correlates similarly by also utilizing the Prandtl and the Reynolds number for correlating the Nusselt number. This correlation has a broader range of validity since it is valid for high turbulent and low turbulent flow. It is valid for Raynolds numbers between $3x10^3$ and $5x10^6$. (Cengel, 2011) The Dropkin and Somerscales correlation is based on the Grashof and the Prandtl number. (Willhite, 1967, p. 3).

3.2 Setup of the simulation

To study the heat exchange capacity a simplified well architecture was simulated. A 7” casing cemented into an 8 1/2” wellbore and completed with a perfectly insulated 3 1/2” tubing. This well architecture was considered suitable to achieve the goal of giving a good impression of a borehole heat exchanger capacity. Properties of the formation are assumed not to change with depth showing a constant thermal conductivity and rock density. Although, in reality of course, the subsurface is stratified. Choosing this approach makes it easier relating the influence of conductivity on power and temperature produced while keeping simulations simple. The thermal gradient is assumed to be 3 Kelvin per 100 meters and constant over depth. The flowrates, inflow temperatures, conductivities, and depth at which the simulations were performed are listed in Table 1.

For the sake of comparison, the parameters for the well architecture, the formation and the completion were kept constant only varying the well depth and the resulting bottom hole temperature.

Table 1: Simulation parameters

Flowrate [m^3/h]	Inflow Temperature [°C]	Depth [m]	Conductivity [W/m^2K]
1	0	1000	2
3	5	2000	2,5
5	10	3000	3
7	15	4000	3,5
9	20	4000	4
11	25	5000	4,5
13	30	6000	5
15	35		
17	40		
19	45		
21	50		
23	55		
25	60		

As mentioned, simulation of the borehole heat exchanger has a transient component in the formation part of the simulation. On a closer look, the result for different simulation parameters was very similar with a characteristic profile like shown in Figure 2. This plot specific shows the simulation results for a well 3000m deep at a flowrate of 15 m^3/h and an inflow temperature of 15°C. In this profile one can easily see, that after a short period of steep decline, a phase of slow decline in temperature and power output follows. The simulation results for an operation of 15 years show that changes in outflow temperature and produced power are minor providing a constant energy level.

For long term business applications, only power constantly available is usable. For this reason, simulation results visualized, discussed, and used for calculations in this thesis, are the ones after 15 years of production.

However, the steep declining curve at the beginning was explained with regards to two thermodynamic properties. The heat conductivity and the heat capacity. While the thermal conductivity of sandstone is low the heat capacity is high. Therefore, the heat stored in the proximity of the borehole, which is directly linked to the high heat capacity, is produced first. After this first period of production of thermal energy production, the heat produced from the wellbore

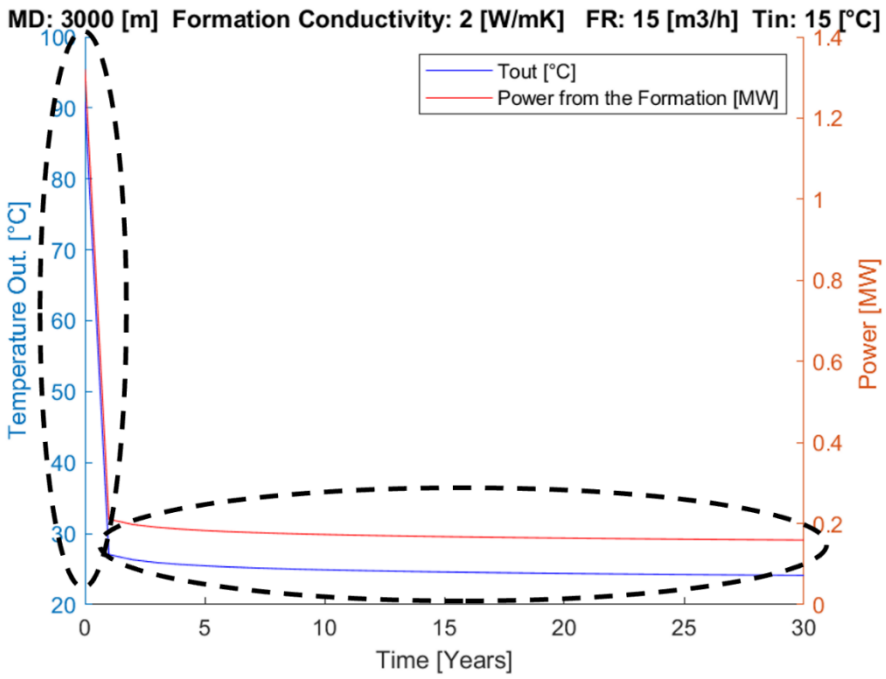

Figure 2: Time dependency of outflow temperature and geothermal power production

is limited to the energy transported through the formation. Thus, the behavior in the flat part of the curve is defined by the heat conductivity of the formation. In figure 2 the respective areas are marked. The conductive dominated production on the left and the capacity dominated production on the right side. Although the short-term effect is not of direct relevance to business applications as researched in this thesis, it might be interesting for applications where only temporary geothermal heat support is needed.

3.3 Visualization of the results

Since the behavior of the heat exchanger is studied in different depth, at different flow rates and under different inflow temperatures there is a verity of data to be processed. Overall, there were 21.294 data points to be visualized, in a way, that trends and capabilities of the borehole heat exchanger at specific well configurations can be evaluated quickly.

The most suitable to visualize the data was found in contour maps. The program used was MATLAB because it provides the user with many different options on the one side to easily handle the mass of Excel data coming from WellUse and on the other side to visualize the data as high-resolution vector graphs. For easier handling, the data was organized in matrixes containing all the data WellUse produced. From these matrixes the data necessary to describe the thermal energy output, the outflow temperature and the hydraulic power requirements were extracted and plotted in contour lines enabling easy understanding and compact display of information. For a better readability and to see occurring tendencies, every value displayed was assigned a different color. This color coding stays consistent throughout all the plots The colors used were carefully selected to make them easily distinguishable while still displaying tendencies in the plots. Because of the many data points sequential color pallets, ordered from low to high were

best suited. Light colors highlight high values and darker colors indicate lower values. For the display of the hydraulic power values the colors were assigned manually to the respective values using RGB triblets. Special attention was given to the areas in the plots which display negative energy levels which means energy is transferred from the fluid into the formation. To be more specific, the negative energy output was covered in grey. Negative energy output is associated with an inflow temperature higher than the outflow temperature. Areas in the plots where the fluid is cooled down are separated with a red line from the areas where the fluid is heated. Described representations can be seen in Figure 3 for an example and in the appendix.

3.4 How to read the tables

The two following examples demonstrate the use of the generic simulation plots to evaluate the potential power and temperature production of a well. From the same plot the pumping power required for circulating the fluid through the borehole heat exchanger can be determined.

Example 1:

Find the outflow temperature, geothermal power output and hydraulic power consumation of a borehole heat exchanger at an inflow temperature of 20°C and a flowrate of 13m^3/h. The formation cunductivity shall be 2 W/mK at a depth of 1000m. The geothermal gradient is 3°C/100m which leads to the undisturbed bottom hole temperature of 44°C.

For solving the excample first the corect table containing information on geothermal power, outflow temperature and hydraulic power has to be found. The correct table can be identified by looking at the bar charts on the right. In figure 3 the bar charts are marked with a dashed line ellipsoid. The correct table for this example is the one showing 2 W/mK at a depth of 1000m and a undisturbed bottom hole temperature of 44°C.

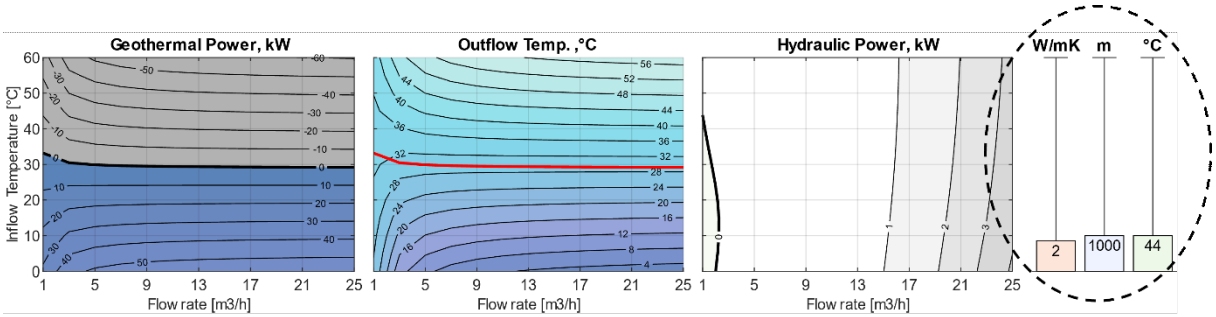

Figure 3: Explanation bar chart

Geothermal power, outflow temperature and hydraulic power have separate windows each and all of them are depictured as a function of flow rate and inflow temperature The ordinate is not shown in each of the three windows but only in the geothermal power window on the very left but is valid for all three windows. Abszissa shows the flowrate in the three windows.

The example is solved by reading the value from the isoenergetic lines in the geothermal power window at 20°C inflow temperature and at a flowrate of 13m^3/h which are marked with red lines in figure 4. The Geothermal power in this excample is at 22 kW.

Next the outflow temperature at a flowrate of 13m^3/h and a inflow temperature of 20°C which are again marked with red lines if figure 4 can be red from the outflow temperature window by comparing the intersection of the red lines with the isothermal lines. The outflow temperature for the example is at 21°C.

The same can be done for the hydraulic power which is 0,85 kW also shown in figure 5.

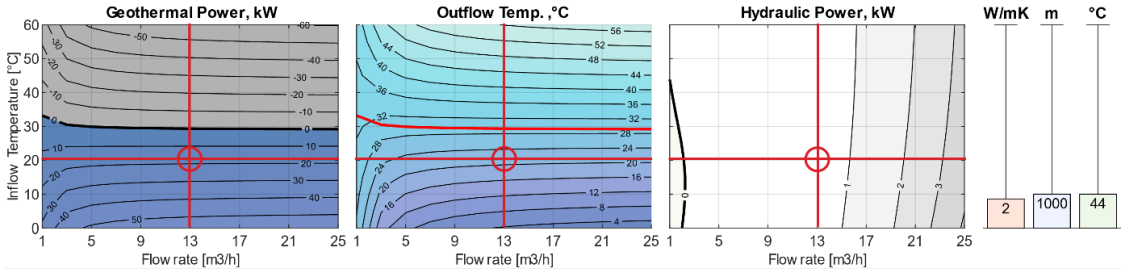

Figure 4: How to read the tables

Example 2:

Find the outflow temperature, geothermal power output and hydraulic power consumation of a BHE at an inflow temperature of 55°C and a flowrate of 17 m^3/h. The formation cunductivity shall be 5 W/mK at a depth of 2000m. The geothermal gradient is 3°C/100m which leads to a undisturbed bottom hole temperature of 74°C.

First the correct table has to be found by looking on the bar chart. Next the lines for inflow temperature and flowrate can be drawn in the three windows. Reading the results at the

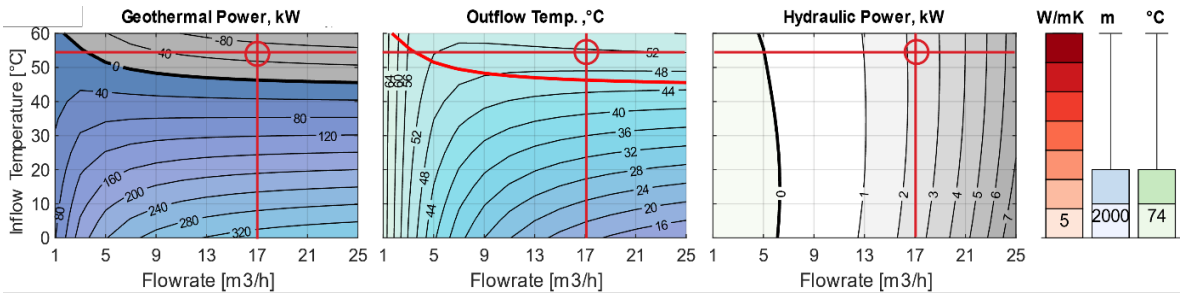

Figure 5: How to read the tables 2

intersection of the lines results in an geothermal power of -60 kW and a outflow temperature of 52 °C. The hydraulic power required to pump fluid through the borehole heat exchanger is 2,2 kW.

Remarkable in example 2 is the negative geothermal power output from the borehole heat exchanger when operated at an inflow temperature of 55°C and a flowrate of 17m^3/h. Operating conditions that result in a negative power output are colored grey in the geothermal power window. Negative geothermal output in this simulation setup is only possible for depth of 1000m and 2000m and happens when the inflow temperature is higher than the outflow temperature from the borehole heat exchanger. Responsible for the negative energy output despite the high undisturbed bottomhole temperature is the temperature progression with depth. Causing the fluid to be cooled down in the upper parts of the well.

To quickly distinguish the areas with a positive from the ones with a negative energy balance the cut off inflow temperature is marked in red in the outflow temperature plot.

4 Interpretation of the results

In general, higher conductivities and temperature differences lead to higher outflow temperatures and geothermal power production. Because the heat flow towards the borehole heat exchanger is higher. Apart from that, two dependencies are important for interpreting the results. First the dependency of produced power and outflow temperature on the temperature difference, between formation and inflow temperature, and second the dependency on the flowrate.

4.1.1 Trends dependent on the temperature difference

As previously mentioned, conductive as well as convective heat transfer strongly depend on temperature difference. This results in low performance in terms of geothermal power output of the borehole heat exchanger at higher inflow temperatures and an increase of the performance as the inflow temperature decreases. In figure 6 the black boxes in the geothermal power window highlight flowrates of 5 m^3/h and 21 m^3/h over the whole range of inflow temperatures. The colors in the boxes brighten as the inflow temperature reduces indicating increasing geothermal power production. The effect repeats for all conductivities and the different depth as it can be seen in the full compendium of graphs attached to this thesis.

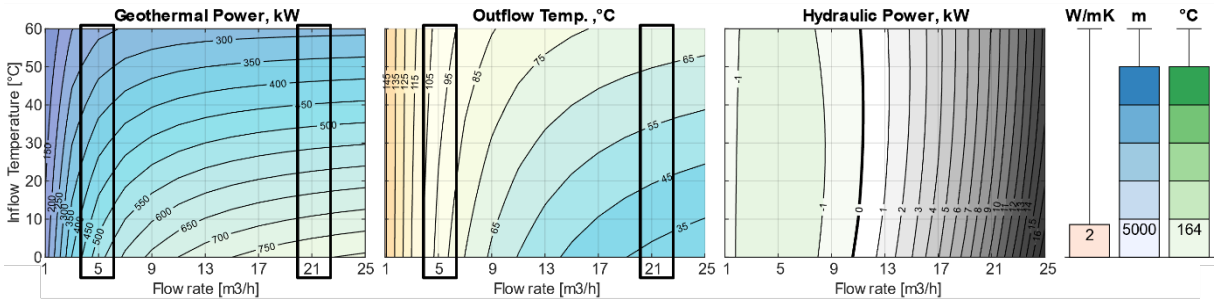

Figure 6: Trends in geothermal power production

This trend also appears in the outflow temperature window where two black boxes in figure 6, again at a flowrate of 5 m^3/h and 21 m^3/h, highlight the behavior. The direction of the trend though is reversed as inflow temperatures rise the outflow temperature increases. This is because the fluids temperature is increased starting from a higher inflow temperature level making it easier to reach higher outflow temperatures. The trend of increasing outflow temperature with increasing inflow temperature weakens with higher flowrates.

4.1.2 Trends dependent on the flowrate

Flow rate is the second factor influencing the geothermal power output because the slower water flows through the system, the higher is its exposure time to the heat flux.

When looking at the boxes in the outflow temperature window at an inflow temperature of 50°C and 20°C in figure 7 the trend becomes visible. As the flowrate decreases the colors become brighter indicating an increase in outflow temperature.

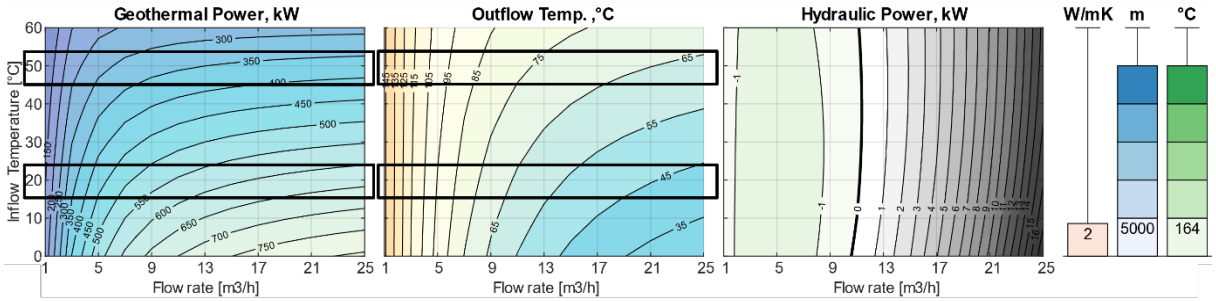

Figure 7: Trends in geothermal power production, FR

Of course, at the same time geothermal power output decreases. This is because lower temperature differences cause a decrease in heat flux again two black boxes in figure 7 mark this behavior.

Increasing exposer time with decreasing flowrates leads to almost vertical lines in areas with low flowrates as marked in figure 7. Temperature differences in these areas are not large enough for upholding a heat flux high enough to substantially increase the geothermal power production.

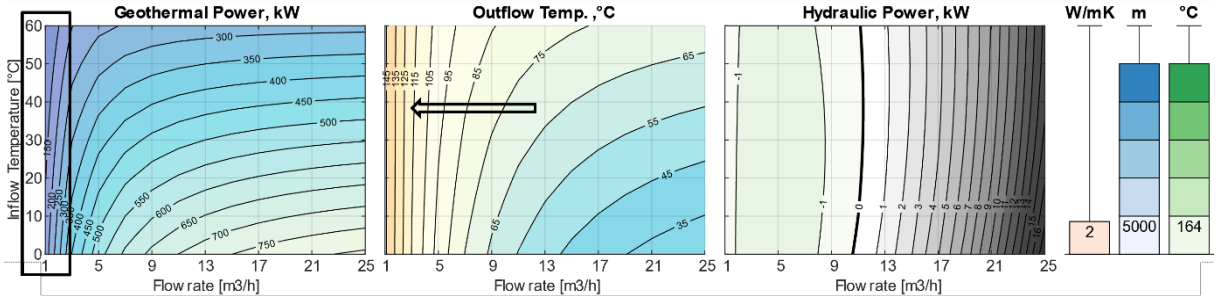

Figure 8: Trends in geothermal power production at low FR

At the same time the outflow temperature is not increasing significantly with decreasing flowrate anymore as indicated by the arrow in the outflow temperature window in figure 8. The lack of heat flux due to low temperature differences causes this.

Both trends combined form the characteristic look of geothermal power window and outflow temperature window throughout all depth and conductivities.

4.1.3 Trends in the hydraulic power

The hydraulic power required to sustain circulation is dependent on the density of the fluid circulated and on the frictional flow behavior.

The density reduces with increasing temperature when fluid is flowing down the annulus and, because for the simulation perfectly insulated tubing is assumed, it stays constant when the fluid flows up the tubing. The higher the temperature difference between the “cool” intake and the “hot” outtake, the higher the density differences and therefore, the lower the required hydraulic power to pump the fluid. This effect is increasing up to a point where the well becomes self-circulating.

Frictional flow behavior is influenced by temperature, the fluid flow velocity and the flow regime. In general friction increases with increasing flowrate.

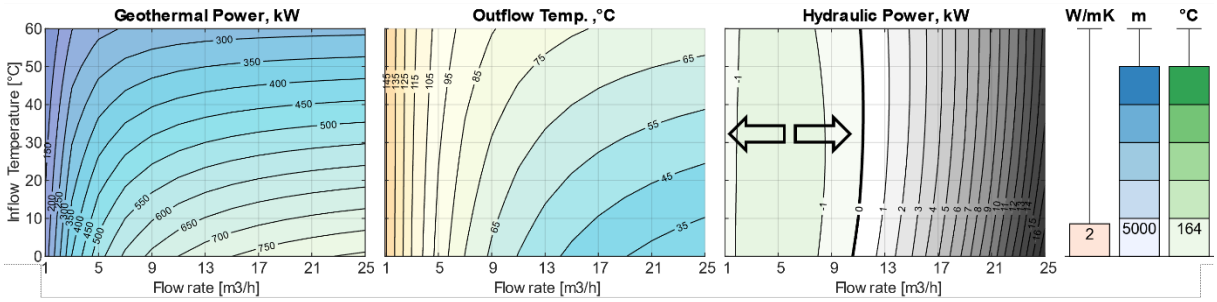

Figure 9: Trends in the required hydraulic power

Shallower wells show a strong dependence of the hydraulic power required on the frictional flow behavior in the annulus and the tubing. At deeper and hotter wells, the tow influencing effects, density differences to frictional behavior get more relevant. The impact of the two opposing effects is indicated with the two arrows in figure 9. The one pointing to the right shows the increase in pumping power with increasing flow rate due to an increase in friction. And the arrow pointing to the left indicates the influence imposed by the density differences to the required hydraulic power.

In the next chapter the practical application of the plots for business applications is explained in examples.

5 Aquaculture

As mentioned before, the temperatures of the geothermal energy produced from oil and gas wells at the end of their lifetime is limited. Thus, finding suitable business opportunities and optimize the system efficiency is crucial for the project profitability.

5.1 Temperature and heat requirements

Table 2 shows boundary conditions in terms of temperature for growing different species. All the shown species are within reduced boundaries and according to the simulation can be produced in most of the wells in the Vienna basin employing the concept of a borehole heat exchanger. Shrimp were investigated closer since there is information on how to grow them available from Güssinger Garnelen[2].

Table 2: Aquaculture temperature requirements (Rafferty, 1991, p. 319)

Species	Lower Min. [°C]	Upper Max. [°C]	Optimal Min. [°C]	Optimal Max. [°C]
Oyster	0	36	24	26
Lobster	0	31	22	24
Shrimp	11	40	25	31
Salmon	4	25	15	15
Catfish	2	35	28	31
Eel	0	36	23	36
Barsch	8	41	22	30
Carp	4	38	20	32
Trout	0	32	17	15
Perch	0	30	22	28

5.2 Power from the borehole heat exchanger

For heating a pond of shrimp hot fluid is produced from the borehole and transferred into the pond where the heat is transferred to the water in the pond cooling the circulation fluid. The geothermal power transferred into the pond depends on the temperature at which the fluid can be produced and the temperature necessary for the shrimp to which the circulation fluid can be cooled down.

[2] https://www.guessinger-garnelen.at/ \last visited 25.02.22

For a shrimp pond it is possible to use the heat coming from the borehole temperature down to a temperature of 1°C above the pond temperature which is at 25°C.

But every higher temperature would also be fine. Calculating those values is hardly possible. Operating experience is required to gather this data. This is because they strongly depend on the design and size of the heat exchanger used for this purpose.

Depending on the temperature requirements an ideal operation point for each application can be found by defining three thresholds.

The first threshold is the need for a positive energy balance. A facility can only be heated if power is produced from the well. Thus, only areas of the geothermal power window and the outflow window below the line separating the two areas are valid. This is shown in Figure 10 below where two arrows point the direction of increasing geothermal power production.

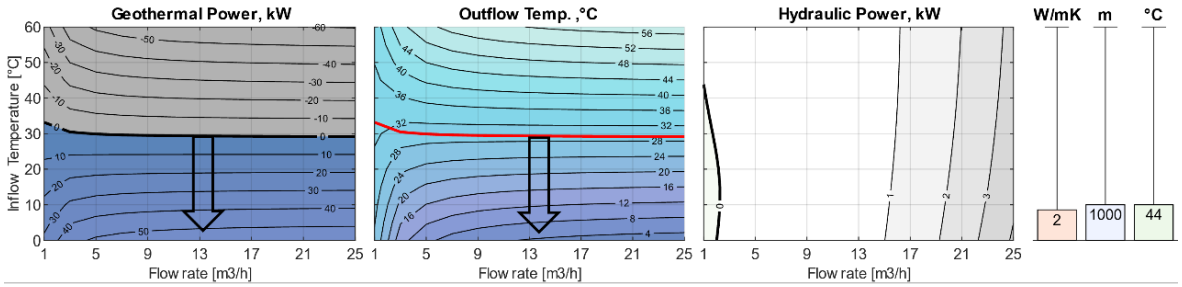

Figure 10: Threshold, positive power balance

The second threshold is the need for the temperature flowing into the borehole heat exchanger to be at or slightly above the temperature a certain application is heated up. The temperature requirement for successful shrimp production is 25°C thus the temperature coming from the borehole heat exchanger can only be used down to this level. In this example the temperature of the fluid flowing back from the shrimp farm into the borehole heat exchanger is at a minimum temperature of 26°C. But as indicated in figure 11 higher return flow temperatures are also fine.

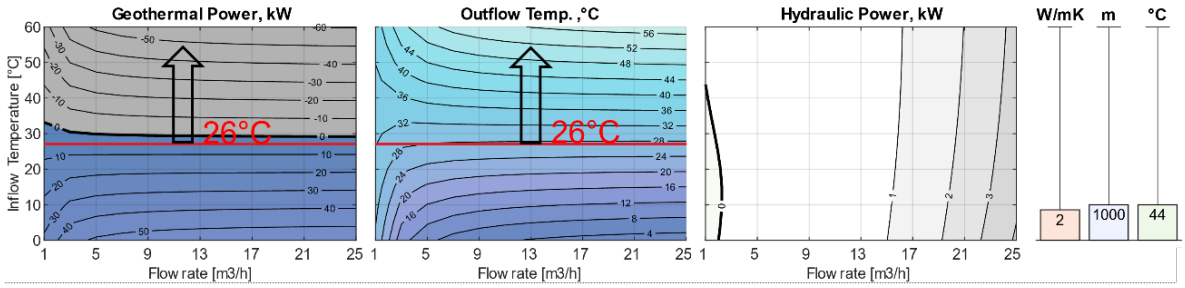

Figure 11: Threshold inflow temperature

The third threshold is the borehole heat exchanger outflow temperature which is in this case 30°C which is 4°C above the 26°C required pond temperature. For this to be fulfilled the regions above the 30°C isotherm in the outflow window are available. The threshold is shown in figure 12.

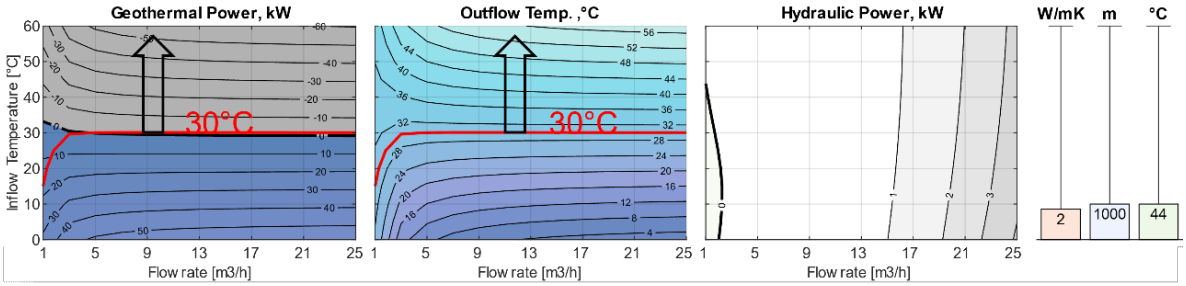

Figure 12: Threshold outflow temperature

When the three thresholds are depicted in one Window, a performance window is created in which a shrimp farm can be operated successfully. The point with the highest energy output is the ideal point of operation. Both the window and the operation point are shown in the geothermal power window in figure 13. The ideal Point of operation is at 5544 W thermal power.

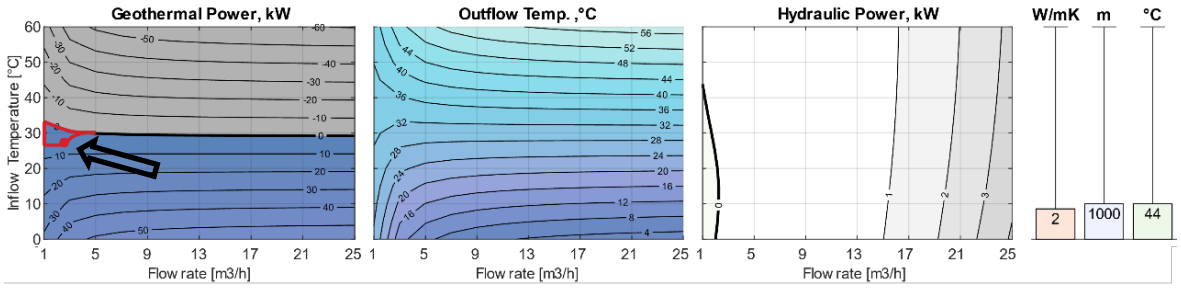

Figure 13: Operation window

In the example determining the amount of pond area which can be maintained throughout the year is now possible. Considering the heating demand of 200 W/m^2 Güssinger Garnelen indicates as requirement for growing Shrimp a total of 28 m^2 of ponds can be heated when a well with a depth of 1000m, 44°C bottom hole temperature and a formation conductivity of 2 W/mK is available. Values used were taken from ponds with a depth of about 1,20m. Areas are used as performance measure, because heat losses restricting the size of such facilities appear mainly on the surface of the ponds. Heat losses are discussed in more detail in chapter 5.3.

Of course, in Summer it is possible to maintain a larger pond-area. But 28 m^2 can be maintained consistent over the whole year. Results for various depth and conductivities are shown in tables 3 to 5. In case of changed operating conditions the potential pond area can be calculated repeating the workflow.

Table 3: Shrimp production from a 1000m deep borehole

Conductivity [W/m^{2}K]	Power [W]	Pond Area [m^2]
2	5544	28
2,5	6796	34
3	8059	41
3,5	9338	47
4	10592	53
4,5	11611	61
5	12688	67

Table 4: Shrimp production from a 2000m deep borehole

Conductivity [W/m^{2}K]	Power [W]	Pond Area [m^2]
2	67 198	354
2,5	81 822	431
3	95 632	503
3,5	108 717	572
4	121 323	639
4,5	133 490	703
5	145 252	726

Table 5: Shrimp production from a 3000m deep borehole

Conductivity [W/m^{2}K]	Power [W]	Pond Area [m^2]
2	186 333	981
2,5	224 139	1 180
3	259 135	1 368
3,5	293 959	1 547
4	326 388	1 718
4,5	357 369	1 881
5	387 020	2 037

5.3 Heating losses in aquacultures

Business unit size is determined by the heat available and the heat consumption of Aquacultures. Table 3 to 5 show that heat available from shallow wells is rather limited. The optimization of pond design and a reduction of the heat demand is crucial. Heat losses of typical ponds used for Aquacultures are discussed in the following as published in (Rafferty, 1991, pp. 319–322). For a typical pond the distribution of heat losses is as presented in table 6.

Table 6: Heat loss distribution (Rafferty, 1991, pp.320)

Heat Loss Method	Amount [%]
Evaporation	37
Convection	31
Radiation	26
Conduction	6

The tendency of the ponds to lose the most energy via evaporation and convection is remarkable.

Evaporation is problematic not because of the volume of water lost but because of the heat removed from the pond when the liquid transforms to gas. The heat required for this process varies with pressure and temperature of the surrounding air. At normal atmospheric conditions it is at 2327 kJ of heat lost per kg of water evaporated from the pond. Evaporation happens even when the temperature of the surrounding air is below the temperature of the pond. Because the driving force for evaporation is the difference in vapor pressure between the surface of the water the surrounding air. When the vapor pressure under a certain air temperature and relative humidity is less than the saturation pressure of the water, evaporation will occur. Generally, at higher water temperatures and lower relative humidity of the air evaporation rates increase (Rafferty, 1991, p. 320).

Convection was already discussed in chapter 2 where it is described as transport of heat associated with particle movement. For aquacultures it is the air exchange rate in the building where the ponds are located, and the temperature of the air passing the water surface. Both is decisive for the magnitude at which losses occur (Rafferty, 1991, p. 320).

Both, evaporation, and convection are strongly influenced by the movement of the surrounding air and the temperature of that air. Evaporation is also influenced by the humidity of the surrounding air. A well-designed housing for the ponds can significantly reduce the heating demand, because it could restrict the movement of the surrounding air and could maintain a high relative humidity above the pond (Cengel, 2011).

Radiative losses are harder to address when it comes to aquacultures then they are usually, and they are also unusually high. Both is because the water surface is radiating to the vapor above it instead of radiation happening between solid bodies. Radiation losses have a high dependency on the difference between the water surface of the pond and the air temperature surrounding the pond. It is hard to restrict radiation losses (Rafferty, 1991, p. 320).

When it comes to aquacultures the concept of thermal mass is useful because the heat capacity of water, 4184 J/kgK, is very high. To give an example at a pond size of 67m^2 and a depth of one meter. The total amount of energy that must be lost to cool down the pond 1K is 280.328 kJ which equals 77,88 kWh. Making it possible to counter peak heating requirements at night by giving up relatively little pond temperature.

Business unit size of aquacultures could easily be increased by utilizing other renewable heating options like solar power. Limiting heat losses using the thermal mass of the pond and adding energy by other means give aquacultures in general a very good chance to be a viable business opportunity for prolonging well life in the Vienna basin. Especially when considering the high market price of shrimp. Which is at 60€/kg according to Güssinger Garneln.

6 Agricultural

Depending on the climate and the crops grown, heating of greenhouses can account for 40% of the cost in greenhouse production of vegetables. Greenhouses are the most popular application for low temperature geothermal energy. Since their ideal temperature requirements lie between 45°C and 85°C, geothermal heated greenhouses are very well suited to produce high value fruits, vegetables and serve as nurseries for a wide variety of plants (Baudoin et al., 2017).

The possibility to use low temperature geothermal wells, however, depends strongly on the mode of heating and the temperature requirements of the crops in the Greenhouse.

6.1 Heating a greenhouse

To keep a relatively constant temperature in the greenhouse, heat that is lost must be fed back into the greenhouse. Heating the lower parts of the greenhouse, where the crops are located is more important, than the space under the roof (Baudoin et al., 2017).

Heat supply with geothermal energy can be treated as heating with any other central heating installation. Important is the placement of the pipes and the temperature level of the heating system. Due to the low temperature difference of the fluid produced from the borehole heat exchanger and the temperature desired a combination of different piping systems may be required. Possible heating mechanisms are.

- Wall pipe coils. The perimeter of the greenhouse is heated. Installations are to be designed in a way that firstly allows the establishment of air currents and secondly does not hinder the entering of light into the building.
- Overhead pipe coils. Since the heat demand closer to the ground and thus to the plants is prioritized it is not the best heating system. But higher plants and facilities in which the prevention of specific plant-diseases is important may require overhead coils.
- In-bed pipe coils. For geothermal heating laying the heating pipes into the plant beds is the preferable method of delivering heat to the plants. The heat is kept very low and close to the plant. This, of course, increases the efficiency.
- Floor pipe coils. They are even more effective than the in-bed piping solution and easier to install and maintain. Especially beneficial for plants grown directly on the floor. Heating closer to the plants reduces the humidity close to them, which is beneficial (Baudion et al., 2013).

Because there are various options for increasing the area of heat exchange heat a greenhouse can be done very efficient.

6.2 Heat demand of a greenhouse

Greenhouses do exist in many different designs and qualities. Finding an easy model to predict the heating demand for any type of greenhouse was key to study the potential for depleted oil

and gas wells in the Vienna basin. A model providing just that, was found in (Hangartner et al., 2010). The model was tested by comparing simulation results to a facility in the Netherlands, and although the heat demand was overestimated a bit, the outcome was fairly accurate and thus applicable for greenhouses in the Vienna basin (Hangartner et al., 2010).

The basis for the model is the SIA 380/1-Thermal Energy in Buildings norm. It deals with the heat losses and gains in the representative energy balances. Calculating the heat demand starts at the mathematical expression for the heat demand of a building in general (Hangartner et al., 2010).

The equations 11 to 15 are used for calculating the heat demand of the Greenhouse. Equation 11 is for calculating the total heat demand of the greenhouse. Equation 12 shows how the conductive heat transfer through the walls is calculated. Equation 13 addresses the heat transfer coefficient needed for calculating conductive heat transfer. One of the limitations of the calculation is neglecting $Q_{internal}$. This means that the heat contribution from machinery and workers inside the greenhouse is ignored (Hangartner et al., 2010). A list of the abbreviations and values used is presented in Table 7.

$$Q_{heating} = (Q_{trans} + Q_{air}) - \alpha(Q_{solar} + Q_{internal})\ [MJ] \quad \text{(Eq. 11)}$$

$$Q_{trans} = \sum k_j A_j (T_{in} - T_{out})\ \ [W] \quad \text{(Eq. 12)}$$

$$k_j = \left(\frac{1}{\alpha_i} + \sum \frac{d_i}{\alpha_i} + \frac{1}{\alpha_{out}}\right)^{-1}\ \ [W/m^2K] \quad \text{(Eq. 13)}$$

$$Q_{air} = nV(\rho c_p)(T_{in} - T_{out})\ [W] \quad \text{(Eq. 14)}$$

$$Q_{solar} = GA_w(f_g \tau f_s)\ \ [W] \quad \text{(Eq. 15)}$$

Determination of the radiation inflow is done using historical values for the solar radiation levels for the location of the greenhouse. Which in the following examples will be Gänserndorf in Austria.

In the calculations although the temperature and thus the heat demand of crops may vary depending on their growing period. Is assumed to be at a constant T_{in} throughout the year. This is because geothermal energy is only useful in greenhouses if the commercial benefit coming from crop growth during the whole year can be utilized.

The average values for the outside temperature T_{out} per month in 2016 in Gänserndorf as well as, for the solar radiation, average values from 2016 in Gänserndorf were taken as input parameters. The results of an example are shown in the figure 17. For the assessment of greenhouse business opportunities, always the power per square meter, and as a second metric the energy per month for a greenhouse with an area of 40.500m and a volume of

162.000 m^3 needed are shown. Both metrics give a good picture of the heat demand on their own right. The calculated area gives a measure of the capabilities of the borehole heat exchanger whereas the energy demand refers to the needs of a greenhouse of realistic size (Baeza et al., 2021, p.36).

Table 7: Parameters for the greenhouse model

Parameters	Symbol	Units	Value
Ground area Greenhouse	A_{ground}	[m^2]	40.500
Volume Greenhouse	V_{tot}	[m^3]	162.000
Area of greenhouse Glass	A_{tot}	[m^2]	112.536
Temperature desired inside	T_{in}	[°C]	17.7
Surface heat transfer coefficients	α_i	[W/m^2K]	8
Conductivity of the window	λ_i	[W/mK]	0.9
Surface heat transfer coefficient	α_{out}	[W/m^2K]	20
Thickness of the window	D_i	[m]	0,0225
Heat transfer through a composite element	K_j	[W/m^2K]	5
Heat exchange number	n	[1/h]	1
Specific volumetric energy constant for air	$\rho\ c_p$	[Wh/m^3K]	0,32
Glass fraction of the glass	f_g	[-]	0,99
Transmittivity of the window	τ	[-]	0,9
Shading factor	f_s	[-]	0,7
Fractional use of heat gains	α	[-]	0,609

A greenhouse with a desired inflow temperate of 17,7°C was calculated using the model described above, to give an example on how typical profiles for outside temperature and solar irradiation profile looks. Which is shown in Figure 17. Also shown are the heating demand of the greenhouse resulting from a desired inside temperature of 17,7°C.

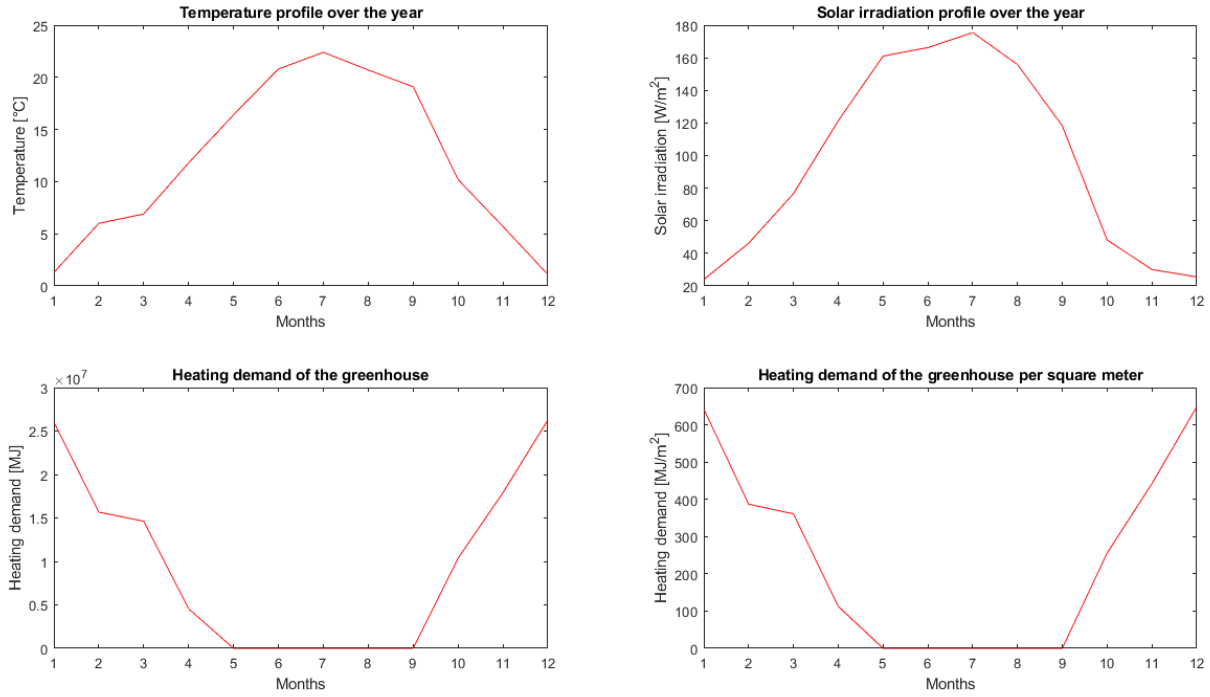

Figure 14: Heating demand over the year according to (Hangartner et al., 2010)

For making the values shown in figure 14 easier legible the energy demand per month for a greenhouse at realistic size and the power demand per square meter are displayed in table 8.

Table 8: Values for greenhouse heating demand over the year according to (Hangartner et al., 2010)

Month	Energy per Month [MJ]	Power per square meter [W/m^2]
January	$2{,}6006\times10^7$	240
February	$1{,}5674\times10^7$	160
March	$1{,}4618\times10^7$	135
April	$0{,}4558\times10^7$	43
May		0
June		0
July		0
August		0
September		0
October	$1{,}0359\times10^7$	95
November	$1{,}7914\times10^7$	171
December	$2{,}6271\times10^7$	242

6.3 Heat exchange in the greenhouse

For choosing the best suited heating system it is important to consider, that no additional heat exchanger between the borehole and the greenhouse heating system is needed. But depending on the wishes of the operator of the greenhouse it may be installed and decrease the heating efficiency. In the following a surface heat exchanger is not considered since the fluid circulated in the borehole heat exchanger is also suited to be circulated in the greenhouse heating system. As more area is dedicated to heating, more heat can be extracted and the higher the efficiency gets. The flowrate is an important design parameter for the heating system in terms of pipe diameter. Efficiency is also influenced by the surrounding temperature and the temperature in the greenhouse as well as the circulation of air inside the Greenhouse. For the following calculations the limitations are considered in terms of temperature. With the borehole heat exchanger inflow temperature being always one degree Celsius above the required inflow temperature and the outflow temperature, from the borehole heat exchanger, being three degrees Celsius above the required minimum temperature. Which is quite within the envelope for the coefficient of performance for such heating systems. When considered, there are no losses in energy generation, and low losses in energy distribution (Hepbasli, 2011, p.4419). Also, should the need for improved performance of the heat exchange in the greenhouse arise, the length of the pipe coils transporting the hot fluid could always be amplified.

Of course, the alteration of plants depending on the season and thus the average outside temperature is beneficial. For the following analysis, to allow better comparison and to stay more on the conservative side. The same plants are simulated to be grown over the whole year.

6.3.1 Tomato

Is economical important, and accounts for over 28% of total vegetable production. Tomatoes are sensitive to frost and require temperatures between 19°C and 24°C during the day and 16°C and 18°C at night. When the temperature level drops below 10°C it is necessary to ensure safe growth of the vegetable. The upper limit for growing tomatoes is 35°C and the day, night difference in temperature must not exceed 6°C (Baudoin et al., 2017).

The relatively high humidity of 65% to 75% is worth mentioning. There are two possible growth cycles available. Half year and full year circle, depending on the capability to control the climate. For the calculation of the heat demand, a necessary greenhouse inside Temperature of 16°C is assumed (Baudoin et al., 2017).

Applying the mentioned temperature-limitations an inflow Temperature into the borehole heat exchanger of 17°C and an outflow temperature of 20°C can be assumed. Resulting in an energy demand as shown in table 9 The size of the greenhouse is assumed to be the same, as in the example shown before.

Table 9: Tomato heat demand

Month	Energy per Month [MJ]	Power per square meter [W/m^2]
January	$2{,}3208 \times 10^7$	214
February	$1{,}3164 \times 10^7$	134
March	$1{,}1820 \times 10^7$	108
April	$0{,}1850 \times 10^7$	18
May	0	0
June	0	0
July	0	0
August	0	0
September	0	0
October	$0{,}7561 \times 10^7$	70
November	$1{,}5206 \times 10^7$	145
December	$2{,}3473 \times 10^7$	216

For better understanding in the tables 10 to 12 the respective area of tomatoes that could be grown with a well available at different depth and at different conductivities is shown. Although simulations down to a depth of 6000m were done only the well-depth down to 3000m are shown since deeper abandoned oil and gas wells are at least very rarely found.

Tables 10 to 12 show the minimum area that can be grown over the whole year and thus are oriented on the maximum energy demand usually occurring in December. However, the heat demand for the whole year is shown in Table 9.

Although geothermal energy is commonly used in greenhouse farming the results for growing tomatoes by using energy harvested by a borehole heat exchanger looks not very promising.

Table 10: Area in m^2 supported by 1000m borehole for growing tomatoes

Formation Conductivity W/mK	Energy, kW	Jan. ,m2	Feb. ,m2	Mar. ,m2	Apr. ,m2	Oct. ,m2	Nov. ,m2	Dez. ,m2
2	22,798	107	170	211	1 267	326	157	106
2,5	27,765	130	207	257	1 542	397	191	129
3	32,562	152	243	302	1 809	465	225	151
3,5	37,244	174	278	345	2 069	532	257	172
4	41,812	195	312	387	2 323	597	288	194
4,5	46,27	216	345	428	2 571	661	319	214
5	50,635	237	378	469	2 813	723	349	234

Table 11: Area in m^2 supported by 2000m borehole for growing tomatoes

Formation Conductivity W/mK	Energy, kW	Jan. ,m2	Feb. ,m2	Mar. ,m2	Apr. ,m2	Oct. ,m2	Nov. ,m2	Dez. ,m2
2	106,198	496	793	983	5 900	1 517	732	492
2,5	128,077	599	956	1 186	7 115	1 830	883	593
3	148,904	696	1 111	1 379	8 272	2 127	1 027	690
3,5	168,802	789	1 260	1 563	9 378	2 412	1 164	782
4	187,864	878	1 402	1 740	10 437	2 684	1 294	870
4,5	206,164	963	1 539	1 909	11 454	2 945	1 422	955
5	223,762	1 046	1 670	2 072	12 431	3 197	1 543	1 036

Table 12: area in m^2 supported by 3000m borehole for growing tomatoes

Formation Conductivity W/mK	Energy, kW	Jan. ,m2	Feb. ,m2	Mar. ,m2	Apr. ,m2	Oct. ,m2	Nov. ,m2	Dez. ,m2
2	242,149	1 132	1 807	2 242	13 453	3 459	1 670	1 121
2,5	290,623	1 358	2 169	2 691	16 146	4 152	2 004	1 346
3	336,314	1 572	2 510	3 114	18 684	4 805	2 319	1 557
3,5	379,552	1 774	2 833	3 514	21 086	5 422	2 618	1 757
4	420,594	1 965	3 139	3 894	23 366	4 805	2 901	1 947
4,5	459,643	2 148	3 430	4 256	25 536	5 422	3 170	2 128
5	496,871	2 322	3 708	4 601	27 604	7 098	3 427	2 300

6.3.2 Cucumber

Cucumber cultivation is at the moment done among other in south east European countries on an area of about 2000 ha in greenhouses and an additional 700 ha under tunnels (Baudoin et al., 2017).

Cucumber is rather sensitive to abiotic and biotic stresses. It is a subtropical plant and thus requires relatively high temperature and humidity. A lot of light and nutrition and temperatures of 22-24°C. The minimum growth temperature is at about 18°C (Baudoin et al., 2017).

Irrigation water-temperature must be controlled, and the soil temperature is also important. But temperature requirements for both do not differ much and are lower than previously mentioned ones. This isbeneficial for when geothermal energy is used as a heat source, as there is also usage for available heat in summer (Baudoin et al., 2017).

Considering temperatures of 18°C as the temperature limit where successful growth is possible. The heat demand throughout the year calculated is as shown in Table 13.

Table 13: Cucumber heat demand

Month	Energy per Month [MJ]	Power per square meter [W/m^2]
January	$2{,}6500\times10^7$	244
February	$1{,}6120\times10^7$	165
March	$1{,}5112\times10^7$	139
April	$0{,}5036\times10^7$	48
May	0	0
June	0	0
July	0	0
August	0	0
September	0	0
October	$1{,}0835\times10^7$	100
November	$1{,}8392\times10^7$	175
December	$2{,}6765\times10^7$	247

Applying an inflow temperature into the borehole heat exchanger of 19°C and an outflow temperature of 22°C wells of different depth and conductivity can deliver as shown in Tables 14 to 16.

Table 14: Area supported by 1000m borehole for growing cucumber

Formation Conductivity W/mK	Energy, kW	Jan. ,m2	Feb. ,m2	Mar. ,m2	Apr. ,m2	Oct. ,m2	Nov. ,m2	Dec. ,m2
2	18,939	78	115	136	395	189	108	77
2,5	23,058	95	140	166	480	231	132	93
3	27,054	111	164	195	564	271	155	110
3,5	30,936	127	187	223	645	309	177	125
4	34,734	142	211	250	724	347	198	141
4,5	38,431	158	233	276	801	384	220	156
5	42,063	172	255	303	876	421	241	170

Table 15: Area supported by 2000m borehole for growing cucumber

Formation Conductivity W/mK	Energy, kW	Jan. ,m2	Feb. ,m2	Mar. ,m2	Apr. ,m2	Oct. ,m2	Nov. ,m2	Dez. ,m2
2	98,521	404	597	709	2 053	985	563	399
2,5	118,878	487	720	855	2 476	1 189	679	481
3	138,252	567	838	995	2 880	1 383	790	560
3,5	156,787	643	950	1 128	3 266	1 568	896	635
4	174,557	715	1 058	1 256	3 637	1 746	998	707
4,5	191,629	785	1 161	1 379	3 992	1 916	1 095	776
5	208,058	853	1 261	1 497	4 335	2 081	1 189	842

Table 16: Area supported by 3000m borehole for growing cucumber

Formation Conductivity W/mK	Energy, kW	Jan. ,m2	Feb. ,m2	Mar. ,m2	Apr. ,m2	Oct. ,m2	Nov. ,m2	Dez. ,m2
2	230,993	947	1 400	1 662	4 812	2 310	1 320	935
2,5	277,331	1 137	1 681	1 995	5 778	2 773	1 585	1 123
3	321,041	1 316	1 946	2 310	6 688	3 210	1 835	1 300
3,5	362,433	1 485	2 197	2 607	7 551	3 624	2 071	1 467
4	401,748	1 647	2 435	2 890	8 370	4 018	2 296	1 627
4,5	439,18	1 800	2 662	3 160	9 150	4 392	2 510	1 778
5	474,889	1 946	2 878	3 417	9 894	4 749	2 714	1 923

6.3.3 Pepper

On the European continent most pepper is grown in Turkey in greenhouses and on fields. Yearly pepper production in Turkey is above 250 000 tons, which is quite a lot. In Greece 5% of all Greenhouse crops-production are pepper. The plant is native to central and south America where it grows during the whole year. Whereas in Europe and Asia it growth annually (Baudoin et al., 2017).

Pepper cultivars are sensitive to temperature level. The air temperature in a greenhouse growing pepper should not exceed 30°C for leaf wilting and fruit browning above that temperature. At daytime temperatures should be between 20°C and 25°C and night temperatures should be between 16°C and 18°C. When the peppers are fruiting higher air temperatures are required. Between 26°C and 28°C during the day and between 18°C and 20°C during the night. The lower limit for greenhouse temperature is 15°C. The average temperature used for calculating the heat demand is therefore at 24°C (Baudoin et al., 2017).

Table 17: Pepper heat demand

Month	Energy per Month [MJ]	Power per square meter [W/m^2]
January	$3{,}6375 \times 10^7$	335
February	$2{,}5040 \times 10^7$	256
March	$2{,}4987 \times 10^7$	230
April	$1{,}4593 \times 10^7$	139
May	$0{,}5873 \times 10^7$	54
June	0	0
July	0	0
August	0	0
September	$0{,}3092 \times 10^7$	29
October	$2{,}0729 \times 10^7$	191
November	$2{,}7949 \times 10^7$	266
December	$3{,}6640 \times 10^7$	338

Growth of pepper takes about 7,5 months. The growth circle can, if necessary, be adjusted to planting in March and harvesting in October to save energy. Because commercial availability over the whole year is important therefore heat consumption over the whole year is considered. Considering an inflow temperature into the borehole heat exchanger of 25°C and an outflow temperature of 28°C wells of different depth and conductivity can deliver what is shown in tables 18 to 20. Table 17 shows the heat demand of peppers throughout the year.

Table 18: Area supported by 1000m borehole for growing pepper

Formation Conductivity W/mK	Energy, kW	Jan. ,m2	Feb. ,m2	Mar. ,m2	Apr. ,m2	May. ,m2	Sept. ,m2	Oct. ,m2	Nov. ,m2	Dez. ,m2
2	8,368	25	33	36	60	155	289	44	31	25
2,5	10,255	31	40	45	74	190	354	54	39	30
3	12,023	36	47	52	86	223	415	63	45	36
3,5	13,743	41	54	60	99	255	474	72	52	41
4	15,436	46	60	67	111	286	532	81	58	46
4,5	17,105	51	67	74	123	317	590	90	64	51
5	18,713	56	73	81	135	347	645	98	70	55

Table 19: Area supported by 2000m borehole for growing pepper

Formation Conductivity W/mK	Energy, kW	Jan. ,m2	Feb. ,m2	Mar. ,m2	Apr. ,m2	May. ,m2	Sept. ,m2	Oct. ,m2	Nov. ,m2	Dez. ,m2
2	75,064	224	293	326	540	1 390	2 588	393	282	222
2,5	91,225	272	256	397	656	1 689	3 146	478	343	270
3	106,283	317	415	462	765	1 968	3 665	556	400	314
3,5	120,73	360	472	525	869	2 236	4 163	632	454	357
4	134,625	402	526	585	969	2 493	4 642	705	506	398
4,5	148,017	442	578	644	1 065	2 741	5 104	775	556	438
5	160,945	480	629	700	1 158	2 981	5 550	843	605	476

Table 20: Area supported by 3000m borehole for growing pepper

Formation Conductivity W/mK	Energy, kW	Jan. ,m2	Feb. ,m2	Mar. ,m2	Apr. ,m2	May. ,m2	Sept. ,m2	Oct. ,m2	Nov. ,m2	Dez. ,m2
2	197,498	590	772	859	1 421	3 657	6 810	1 034	743	584
2,5	237,434	709	928	1 032	1 708	4 397	8 187	1 243	893	703
3	275,206	822	1 075	1 197	1 980	5 096	9 490	1 441	1 035	814
3,5	311,068	929	1 215	1 353	2 238	5 761	10 726	1 629	1 169	920
4	345,216	1 031	1 349	1 501	2 484	6 393	11 904	1 807	1 298	1 021
4,5	377,806	1 128	1 476	1 643	2 718	6 997	13 028	1 978	1 420	1 118
5	408,968	1 221	1 598	1 778	2 942	7 574	14 102	2 141	1 538	1 210

6.3.4 Eggplant

Turkey is the main producer with a cumulative production of 180 000 tons per year. The plant originally comes from India (Baudoin et al., 2017).

The optimal growing temperature is between 21°C and 30°C with the upper limit for growth at 40°C. The lower temperature limit is at 10°C. The plants need a lot of light. This is why from the two available production cycles usually the one from February to July is chosen. Because commercial availability over the whole year is important heat consumption over the whole year is assumed (Baudoin et al., 2017).

The resulting heat demand for growing eggplant at 21°C are shown in Table 21.

Table 21: Eggplant heat demand

Month	Energy per Month [MJ]	Power per square meter [W/m^2]
January	$3{,}1438 \times 10^7$	300
February	$2{,}0580 \times 10^7$	210
March	$2{,}0049 \times 10^7$	184
April	$0{,}9814 \times 10^7$	93
May	$0{,}0936 \times 10^7$	9
June	0	0
July	0	0
August	0	0
September	0	0
October	$1{,}5791 \times 10^7$	145
November	$2{,}3171 \times 10^7$	221
December	$3{,}1703 \times 10^7$	292

Considering an inflow temperature into the borehole heat exchanger of 22°C and an outflow temperature of 25°C wells of different depth and conductivity can deliver what is shown in the tables 22 to 24. Unfortunately, the heat demand is rather high. Growing eggplants with only geothermal energy using a borehole heat exchanger seems not very promising. Even growth cycles from February to July are not promising.

Table 22: Area supported by 1000m borehole for growing eggplant

Formation Conductivity W/mK	Energy, kW	Jan. ,m2	Feb. ,m2	Mar. ,m2	Apr. ,m2	May. ,m2	Oct. ,m2	Nov. ,m2	Dez. ,m2
2	13,404	45	64	73	144	1 489	92	61	46
2,5	16,3	54	78	89	175	1 811	112	74	56
3	19,125	64	91	104	206	2 125	132	87	65
3,5	21,877	73	104	119	235	2 431	151	99	75
4	24,541	82	117	133	264	2 727	169	111	84
4,5	27,171	91	129	148	292	3 019	187	123	93
5	29,73	100	142	162	320	3 303	205	135	102

Table 23: Area supported by 2000m borehole for growing eggplant

Formation Conductivity W/mK	Energy, kW	Jan. ,m2	Feb. ,m2	Mar. ,m2	Apr. ,m2	May. ,m2	Oct. ,m2	Nov. ,m2	Dez. ,m2
2	86,99	290	414	473	935	9 666	600	394	298
2,5	105,148	350	500	571	1 130	11 672	725	475	360
3	122,269	408	582	665	1 315	13 585	843	553	419
3,5	138,76	463	661	754	1 492	15 418	957	628	475
4	154,592	515	736	840	1 662	17 177	1 066	700	529
4,5	169,824	566	809	923	1 826	18 869	1 171	768	582
5	184,502	615	879	1 027	1 984	20 500	1 272	835	632

Table 24: Area supported by 3000m borehole for growing eggplant

Formation Conductivity W/mK	Energy, kW	Jan. ,m2	Feb. ,m2	Mar. ,m2	Apr. ,m2	May. ,m2	Oct. ,m2	Nov. ,m2	Dez. ,m2
2	214,248	714	1 020	1 164	2 304	23 805	1 478	969	734
2,5	257,385	858	1 226	1 399	2 768	28 598	1 775	1 165	882
3	298,125	994	1 420	1 620	3 206	33 125	2 056	1 349	1 021
3,5	336,751	1 223	1 604	1 830	3 621	37 417	2 322	1 524	1 153
4	373,482	1 245	1 779	2 030	4 016	41 498	2 576	1 690	1 279
4,5	408,491	1 362	1 945	2 220	4 392	45 388	2 817	1 848	1 399
5	441,926	1 473	2 104	2 402	5 752	49 103	3 048	2 000	1 513

6.3.5 Lettuce

Lettuce is rather well suited to be grown in cooler environments. If falls under the group of leafy vegetables like endive, chicory, lamb´s lettuce, spinach, and Swiss chard. All of them are well known in Austria and consumed commonly (Baudoin et al., 2017).

Temperatures ideal to grow lettuce are at 23°C during the day and °7 at night which makes an average temperature of 15°C. But average temperatures of 14°C or 13°C are also quite possible. The lower temperature limit is near the freezing point (Baudoin et al., 2017).

Table 25 shows the energy demand at a greenhouse inside temperature of 14°C.

Table 25: Lettuce heat demand

Month	Energy per Month [MJ]	Energy needed per square meter [W/m^2]
January	$1{,}9916 \times 10^7$	184
February	$1{,}0173 \times 10^7$	104
March	$0{,}8528 \times 10^7$	79
April	0	0
May	0	0
June	0	0
July	0	0
August	0	0
September	0	0
October	$0{,}4269 \times 10^7$	39
November	$1{,}2021 \times 10^7$	115
December	$2{,}0181 \times 10^7$	186

The temperature for inflow into the borehole heat exchanger is set at 15°C and the outflow temperature is assumed to be at a minimum of 18°C. Out of the presented plants that can be grown in greenhouses lettuce is the most promising one. This is due to its high resilience to temperature changes and the broad range of temperatures at which it can be grown. Tables 26 to 28 show the potential for growing lettuce.

Table 26: Area supported by 1000m borehole for growing lettuce

Formation Conductivity W/mK	Energy, kW	Jan. ,m2	Feb. ,m2	Mar. ,m2	Oct. ,m2	Nov. ,m2	Dec. ,m2
2	26,719	145	257	338	685	232	144
2,5	32,533	177	313	412	834	283	175
3	38,173	207	367	483	979	332	205
3,5	43,663	237	420	553	1 120	380	235
4	49,017	266	471	620	1 257	426	264
4,5	54,247	295	522	687	1 391	472	292
5	59,364	323	571	751	1 522	516	319

Table 27: Area supported by 2000m borehole for growing lettuce

Formation Conductivity W/mK	Energy, kW	Jan. ,m2	Feb. ,m2	Mar. ,m2	Oct. ,m2	Nov. ,m2	Dec. ,m2
2	113,875	619	1 095	1 442	2 920	990	612
2,5	137,287	746	1 320	1 738	3 520	1 194	738
3	159,556	867	1 534	2 020	4 091	1 387	858
3,5	180,817	983	1 739	2 289	4 636	1 572	972
4	201,171	1 093	1 934	2 547	5 158	1 750	1 082
4,5	220,698	1 199	2 122	2 794	5 659	1 919	1 187
5	239,465	1 301	2 303	3 031	6 140	2 082	1 287

Table 28: Area supported by 3000m borehole for growing lettuce

Formation Conductivity W/mK	Energy, kW	Jan. ,m2	Feb. ,m2	Mar. ,m2	Oct. ,m2	Nov. ,m2	Dec. ,m2
2	253,305	1 377	2 436	3 206	6 495	2 203	1 362
2,5	303,915	1 652	2 922	3 847	7 793	2 643	1 634
3	351,587	1 911	3 381	4 451	9 015	3 057	1 890
3,5	396,672	2 156	3 814	5 021	10 171	3 449	2 133
4	439,439	2 388	4 225	5 563	11 268	3 821	2 363
4,5	480,106	2 609	4 616	6 077	12 310	4 175	2 581
5	518,854	2 820	4 989	6 658	13 304	4 512	2 790

6.4 Economics of greenhouse farming

The potential for greenhouse farming addressed in square meters is not very promising for wells with a depth lower than 2000 meters. In the following a short economic analysis underlining this statement is executed.

Using geothermal power for greenhouse farming serves the purpose of extending the growing period for the plants over the whole year. Economics of greenhouses in this context must be addressed as the potential for growing them over the whole year. For assessing the potential greenhouses could have the plant yield per square meter and the revenue that could be generated by selling them are determined from literature. Depending on the results the feasibility of greenhouses serving as a viable business opportunity can be estimated.

For tomatoes the average crop yield per year is at 16 kg/m^2. Market prices are changing over the year. In 2021 market prices were highest in March. Having these two numbers the revenue in €/m^2 can be calculated. Considering the maximum m^2 that can be heated over the whole year a reasonable number for the revenue a greenhouse facility would generate can be calculated. These economic boundaries are summarized in table 29.

Table 29: Economic boundary conditions for different crops

Vegetable	Crop yield per year	market prize	Revenue	Literature for crop yield
Tomatoes[3]	16 kg/m^2	1,67 €/kg	26,72 €/ m^2	(Hatirli et al., 2006, p. 433)
Cucumber[4]	12 kg/m^2	0,68 €/kg	8,16 €/ m^2	(Mohammadi and Omid, 2010, p. 195)
Pepper[4]	12 kg/m^2	3 €/kg	36 €/ m^2	(Fernández et al., 2005, p. 1)
Lettuce[4]	11 pc/m^2	0,72 €/pc	7,92 €/ m^2	(Engindeniz and Tuzel, 2006, p. 288)

[3] https://ec.europa.eu/info/food-farming-fisheries/farming/facts-and-figures/markets/overviews/market-overview-sector_en \last visited 22.02.22

[4] https://www.ama.at/marktinformationen/obst-und-gemuse/marktbericht \last visited 22.02.22

For tomatoes the maximum revenue calculated in this way is 6.252€ per year. For a well with a depth of 1000m and a formation conductivity of 5 W/mK and thus an available area of 234m^2. It can be hardly believed that a facility of this size can be profitable.

Especially when considering that additional heating by mounting solar panels on the roof of the structure is not possible. For the sake of comparison. A full-time business for only one person would require an area of at least 560 square meters[5]. The average size for greenhouses in the Netherlands is about 50 000m^2 (Baeza et al., 2021, p.36).

Results for growing tomatoes utilizing a well 2000m deep with a formation conductivity of 5 W/mK, which is the highest conductivity used for simulations are also not very promising. With an area of 1.036m^2 used for growing tomatoes a revenue of 27.682€ per year could be generated. Even a 3000m deep wellbore with a conductivity of 5W/mK offering 2300 m^2 does only generate 56.860€.

Financial assessment for the other crops presented in tables 30 to 32 does not show much better results. When the revenue of different crops grown with the energy coming from wells of different depth and a formation conductivity of 5W/mK is calculated.

Table 30: Revenue from a 1000m deep well with a conductivity of 5 W/mK

Plant	Area for Farming, m^2	Revenue, €
Tomatoe	234	6 252
Cucumber	170	1 387
Pepper	55	1 980
Lettuce	319	2 526

Table 31: Revenue from a 2000m deep well with a conductivity of 5 W/mK

Plant	Area for Farming, m^2	Revenue, €
Tomatoe	1 036	27 682
Cucumber	842	6 871
Pepper	476	17 136
Lettuce	1 287	10 193

[5] https://www.homeadvisor.com/cost/outdoor-living/build-a-greenhouse/ \last visited 21.02.22

Table 32: Revenue from a 3000m deep well with a conductivity of 5 W/mK

Plant	Area for Farming, m^2	Revenue, €
Tomatoe	2 128	56 860
Cucumber	1 923	15 692
Pepper	1 210	43 560
Lettuce	2 790	22 097

Out of the different assessed tomatoes are the most profitable but still cannot reach the area a greenhouse usually has. And the revenues are very low.

7 Bio methane

In the foreseeable future the demand for methane especially in the industry remains high. Domestic production of CO_2 neutral Methane is rather low until today. [6]

Bio-methane production is technically a carbon neutral process in which organic matter in a specific environment, is converted into CH_4. However, the biggest advantages hydrocarbons have is their high energy density and the possibility to be transported and stored relatively easy, disappears in conventional Bio Methane production facilities. This is because the produced gas is converted into thermal and electrical energy by a connected small-sized caloric plant. A part of the converted energy is used to create the necessary temperature environment for the transformation of organic waste into Methane (Utinger et al., 2019).

Table 33 gives information about the energy demand and the output of typical Bio-methane production facilities.

Table 33: Biogas facilities overview (Utinger et al., 2019)

Facility type	Material [kt/a]	Material type	Thermal own consumption [%]	Power output elect. [kWel]
Small agricultural facility	<5	Mainly slurry	40-60	30-60
Medium size agricultural facility	8-15	fertilizer and substrate	30-40	150-200
Large agricultural facility	20-30	fertilizer and substrate	25-35	300-500
Industrial facility	20-30	green waste and industrial waste	10-30	400-1000

As a rule of thumb one can say, that one ton of corn leads to a production of about 200 m^3 of Biogas with a Methane content of about 52%. The exact amount of Methane produced is of course dependent on the process parameters.[7]

[6] https://www.derstandard.at/story/2000127086752/oesterreich-muss-auch-bei-erneuerbarem-gas-auf-das-ausland-hoffen \last visited 29.01.2021 \last visited 04.02.2022

[7] https://www.heizungsfinder.de/bhkw/biogasanlage/substrate/faustzahlen \last visited 04.02.2022

7.1 Principles of biogas production

Biogas refers to the gas produced in a biogas plant, whatever constituents this gas may have. Biomethane on the other hand or upgraded biogas is the clean product, that has higher Methane content that depends on the regulations in place (Tabatabaei and Ghanavati, 2018, p. 240). Other constituents then methane are carbon dioxide, oxygen, water, sulfur, ammonia and hydrogen sulfur (H_2S). Where the main constituents are CO_2 with a share of 30% to 50%, CH_4 with a content that fluctuates between 50% and 70% (Tabatabaei and Ghanavati, 2018, p.239).

The formation of biogas from organic matter is a process occurring in nature, and if not controlled converts organic matter into the before mentioned Molecules. Due to high methane output in the biomass decay and the high contribution of methane to global warming, capturing, and utilizing the methane in a controlled environment is a good idea (Tabatabaei and Ghanavati, 2018, p. 120). Since the 1930s biogas was produced and the process was over time professionalized. Up to the industrialized plants that nowadays can be found (Klinghoffer and Castaldi, 2013, p. 368). Biogas productions is most commonly used in Europe whereas Germany is most ambitious due to efforts of lawmakers to reduce carbon emissions (Klinghoffer and Castaldi, 2013, p.369).

7.1.1 Biogas generation-the process

As mentioned, biogas generation is a process occurring in nature or in an controlled anaerobic environment under specified temperature conditions as a in a plant. There are some basic conditions under which a Biogas generation process is efficient.

- air is to be absent,
- temperature must be constant and uniform,
- there must be optimal nutrient support,
- the pH must be uniform and adjusted (Tabatabaei and Ghanavati, 2018, pp. 137–138)

Most interesting for the intended supply of the biogas plants with geothermal energy from abandoned oil wells is the temperature on which they operate. When the degradation process happens between 30°C and 42°C the environment is called mesophilic. If the process happens in a temperature range between 43°C and 55°C it is called thermophilic. The lower temperature limit is at 30°C and the upper limit is at 57°C. A higher temperature speeds up the degradation of the substrate and thus the whole process (Tabatabaei and Ghanavati, 2018, p.138).

7.2 Meeting the heat demand of a biogas plant

The heat and the electricity demand of a plant depend on the temperature level it is run, the geometry, and of course the ambient temperature.

Heating demand of a plant differs relatively strongly depending on the facility type. Better insulation with e.g. stone wool reduces the heating demand, but increases costs. This can be used as an advantage, as the plant when designed from scratch can be adjusted to the heating a adjacent geothermal well could provide (Klinghoffer and Castaldi, 2013, p. 240). Values for the heating demand of biogas production facilities can be found in (Kleine Mölle and Dürr, 2016). Values there show, that up-to-date plants use around 28% of the produced energy for thermal own consumption. Further a mesophilic environment is assumed setting the temperature within 32°C to 42°C. Considering, that the heat transfer into the plant is executed by pipes running through plant. The heating system can be designed efficiently depending on the heat exchange system between the borehole fluid and the biogas plant. Losses during heat exchange can go up to 10% of the supplied heat (Klinghoffer and Castaldi, 2013, p.249).

A mesophilic environment at a temperature of 35°C is considered. From the available heat then the capacity for the Biogas facility is calculated in terms of biogas that can be produced. A second measure is the amount of biomethane that can be produced. Usually 9,968 [kWh/m^3] (Kleine Mölle and Dürr, 2016) Also during upgrading the biogas some losses of around 5% occur that need to be considered. (Kleine Mölle and Dürr, 2016) For meeting the heat demand of the facility at an operating Temperature of 35°C the fluid is considered to leave the borehole heat exchanger at a temperature of 38°C and be circulated back at a temperature of 36°C. The temperature difference is kept at a minimum to reflect the necessity of maintaining the biogas facility at minimum temperature difference. Boreholes at a depth of 1000m are unfortunately not able to meet the temperature requirements of a biogas facility. Thus, starting with boreholes with a depth of 2000m volumes of biomethane produced were calculated. From the available heat the energy produced from the plant was calculated by assuming a thermal own consumption of 28%. Then accounting for the losses of 10% subsequently calculating the volume of methane that can be produced and accounting for upgrading losses of 5%.

Table 34: Biogas production from a 2000m borehole per year

Formation Conductivity W/mK	Heating Energy, kW	Energy delivered, kW	Volume Biomethane, sm^3/a
2	33,510	107,710	17 985
2,5	40,803	131,150	21 899
3	47,879	153,900	25 697
3,5	54,765	176,030	29 392
4	61,532	197,800	33 024
4,5	68,193	219,200	36 600
5	74,716	240,160	40 100

Table 35: Biogas production from a 3000m borehole per year

Formation Conductivity W/mK	Heating Energy, kW	Energy delivered, kW	Volume Biomethane, sm^3/a
2	122,524	437,585	73 070
2,5	147,931	925,600	88 220
3	172,160	1.077,2	102 670
3,5	195,344	1.222,3	116 490
4	217,585	1.361,5	129 750
4,5	238,961	1.495,2	142 500
5	259,540	1.624,0	154 770

The results show in tables 34 and 35 when compared with table 33 that heat from the borehole heat exchanger can sufficiently supply a biogas facility of small size. However, applications where the facility is only supplied partially by geothermal energy are more likely to be realized.

8 Aquifer thermal energy storage

Previously within the framework of this thesis discussed applications were dealing with using the abandoned well only. For the Aquifer Thermal Energy Storage (ATES) it is quite the opposite. The concept exists in different versions for different depth and temperatures, but essentially the goal is always, to store energy in the form of heat in subsurface aquifers. Utilizing not only the Well itself to produce energy from the formation, but also utilizing the adjacent aquifer enables the creation of a relatively efficient energy storage. Unlike batteries, aquifers allow storage of energy over longer times, but lack the ability to act on the short term. Thus, making them the ideal solution in compensating seasonal mismatch of energy production and consumption (Fleuchaus et al., 2018, p.861).

The basic principle is very easy to understand. Two wells are connected to an aquifer between them. When hot water from a surface plant is available this water is injected into the “hot” well and cold water is produced from the “cold” well, heated at the surface and re-injected. When heat is needed, the injection direction is changed and cold water is injected into the cold well and the warm water is re-produced from the hot well.

Most experience exists in low enthalpy, low depth applications used for domestic heating (Fleuchaus, 2020, p. 20) (Bakima et al., 2019). Higher Enthalpy ATES above an operating temperature 95°C are considered to be experimental. (Bakima et al., 2019) They are of course interesting because high enthalpy storages, at least in theory, would allow for generating electricity from the produced high enthalpy reservoir fluid. Thus help closing the gap between winter and summer electricity production (Fleuchaus, 2020, p. 61). ATES setups that would allow for this are not the focus here since are considered experimental and not much information is available in literature. Nevertheless, for future developments high enthalpy ATES may very well be a business opportunity to catch on to.

8.1 History and basics of ATES

Development of ATES is going on for a long time. With the first known applications in Shanghai back in the 1960s when the local textile industry used the storage capabilities of groundwater aquifers to cool their facilities. Research and development intensified in Europe and North America as a reaction on the oil crisis in the 1970s striving the commercialization of higher temperature storages for heating purposes. Difficulties like clogging, corrosion, buoyancy flow, thermal breakthrough and clay swelling caused a shift towards lower temperature applications. The Netherlands is nowadays the country where most applications can be found. Utilizing aquifers for heating purposes is easy there because a lot of the aquifers are saline and not used for drinking water production (Fleuchaus et al., 2018, p.866).

ATES are commonly subdivided into low temperature (LT), sometimes medium temperature (MT) applications and high temperature (HT) applications. Where to draw the border between the different categories different opinions can be found in literature. Different categorization happens because of different criteria. Legally it comes in handy to define the boundaries

according to the maxim allowed injection temperature which is between 18°C and 25°C in Europe. Whereas from a technical standpoint it is better to have a threshold at 50°C. This is the temperature below which usually water treatment is unnecessary because problems like buoyancy flow, scaling and corrosion do not appear. Another measure is the applicability of the produced fluid for heating purposes defined by the thermal isolation of the heated buildings. Or the requirements of the district heating network which of course differs. Table 36 presents a common classification. With the separation between medium and high temperature being set at 50°C (Fleuchaus, 2020, pp.54–55) but separation at 60°C is also possible (The 12th International Conference on Energy Storage, 2012, p. 1). However the classification storing energy at high temperatures efficiently without touching the groundwater was decided to be of most interest is thus discussed in this thesis by the means of an actual project and discussing recent research.

Table 36: ATES classification

Low Enthalpy	Medium Enthalpy	High enthalpy
<30°C	30-50°C	>50°C

In terms of research the HEATSTORE project [8] carried out by different renowned universities and companies proved to be a valuable source of information. Another good source of information were publications from the Karlsruhe Institute of Applied Geothermics with their research project concerning the utilization of abandoned hydrocarbon reservoirs for deep geothermal heat storage.

8.2 Neubrandenburg

In Neubrandenburg two district heating systems supply most of the buildings with heat. The larger supply system is supplied with heat from a combined heat and power plant (CHP) driven by a gas and steam turbine. The baseload of the plant is at 77MW electricity and 90MW heat. The network provides a heating capacity of 200MW. The feeding temperature is 130°C and the return flow temperature is 60°C. (Kabus et al., 2005, p.1) In winter the efficiency of the combined heat and power production was almost 90%. Whereas in summer the heat demand was too low and the return flow temperature too high to reach such good efficiencies (Zenke et al., 2000, p.1).

The second smaller system was supplied from a geothermal plant between 1987 to 1998. The geothermal heating plant (GHP) consisted out of 2 doublets producing from the Hettingen/Upper Postera horizons at a depth between 1200m and 1300m with a flowrate of 150m^3/h. The temperature of the produced water was between 53°C and 55°C with a mineralization of 120-130 g/l. The heating capacity of the smaller network is 12MW.

[8] https://www.heatstore.eu/ \last visited: 01.02.2022

The feeding temperature is 80°C and the return flow temperature is 45°C. Due to the low temperature of the water produced from the GHP absorption type heat pumps had to be used for meeting the heat demand making the system inefficient (Kabus et al., 2005, p.1).

When in 1998 due to corrosion damage on unprotected metal pipes and because of oxygen entering the water cycle the GHP was inoperative. It was decided to transform the GHP to an ATES (Vetter et al., 2012, p.9). The concept developed addressed the efficiency problems in the GHP plant and the loss of the GHP. With the access heat from the GHP in summer being first transported through the district heating system. If not used after being transported to the former GHP the heat would be stored in the ATES. The feeding temperature was planned to be 80°C and the flowrate was planned to be 80m^3/h. In winter production temperatures between 80°C and 65°C were anticipated. The water then produced was intended to be run as before but with higher temperatures. It was calculated, that between April and September 12.000 MWh of heat would be fed into the storage and that in winter about 8.800 MWh could be produced from the ATES, resulting in an efficiency of 72%. The heat production rate was estimated to be between 4,0 and 2,9 MW (Kabus et al., 2006).

It was decided to use the former production well GtN1 as the hot well and the former injection well GtN4/86 as the cold well (Wolfgramm and Seibt, 2006). Meaning, that in summer cold water is produced from the GtN4/86 and warm water is injected into the GtN1 well. In winter hot water is produced from the GtM1 well and cold water is injected into the GtN4/86 well (Wolfgramm and Seibt, 2006).

The decision to use these two wells was made despite the fact that originally the GtN1 well was connected to the deeper upper Postera formation, and the GtN4/86 well was connected to the shallower Hettangian Upper bank formation. Connecting both wells to the Upper Postera formation was done by extending the GtN4/86 well 100m to a TVD of 1270m. The GtN1 has a TVD of 1285m (Zenke et al., 2000, p.4). Because the injection well from the geothermal doublet GtN1 was a part of is only 1-2m away from the new GtN4/86 connection to the Upper Postera formation this makes sense. The well previously used for injection was cemented back (Wolfgramm and Seibt, 2006).

Postera formation had a reservoir temperature of 54°C before the storage operation started a thickness between 15m and 20m. The porosity is between 20-25% the sediments were deposited under a channel-like deltaic environment (Vetter et al., 2012, p.9).

On the surface most of the facilities remained unchanged except of some by-passes around filters. The by-passes had to be installed to allow for injection and production. Also installation on the wellheads were changed to glass reinforced plastic made products. For additional safety a Nitrogen system to pressurize the annulus was installed. The wells were recompleted to withstand the requirements in terms of corrosion and flowrate. As well as to support the altering production and injection cycles at a flowrate of 100 m^3/h. The system was at a reservoir pressure of 130 bar and surface pressures between 2bar and 6 bar. (Vetter et al., 2012, p.9) In figure 15 the completion design is shown (Kabus et al., 2006).

After recompletion was done an intense testing program including injection-, production-, and circulation test was carried out. In March 2004 the test run started with an injection period. Injection temperature was at first 70°C and continuously increased up to a temperature of 78°C. Injection was continued until the end of October 2004. After 3 month of delay production from the ATES started in January. An amount of 10.000MWh was stored and 3.000MWh were produced in the test run. In March 2005 regulatory operation started with an injection period the first production period starting in November 2005 (Kabus et al., 2006).

The first injection and production cycle are shown in detail in figures 16 and 17. Figure 16 shows the temperatures at the wellhead for the cold and the warm well, Figure 17 shows the heating power injected and produced over the first circle. Throughout the operation in summer water was produced from the cold well with temperatures between 54°C and 45°C subsequently filtered and transported and heated of to injection temperature. In between the fluid is filtered twice once after production and ones before injection. The injection temperature was increased throughout the operation. From 2005 to September 2009 the injection temperature was 80°C. Later it was raised to 85°C (Vetter et al., 2012, p.9). The production temperature in winter mode changes as the discharge proceeds. With initial temperatures of around 80°C decreasing down to temperatures of 65°C. With the injection temperature changed to 85°C the production temperatures did not fall below 70°C After going through an heat exchanger the water was injected in the cold well (Vetter et al., 2012, p.9).

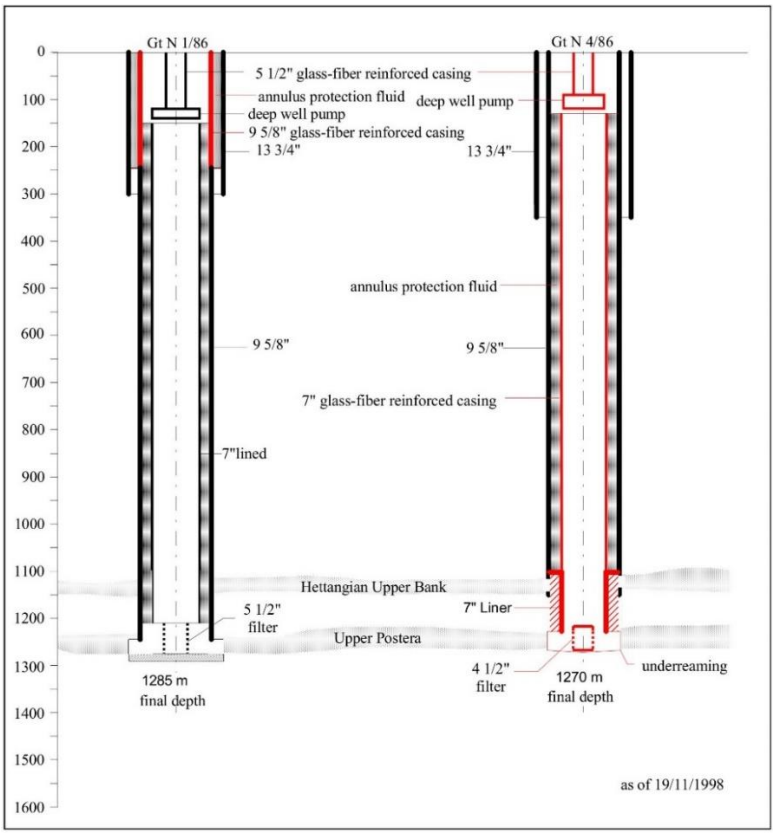

Figure 15: Completion design Neubrandenburg (Zenke et al., 2000, p.4)

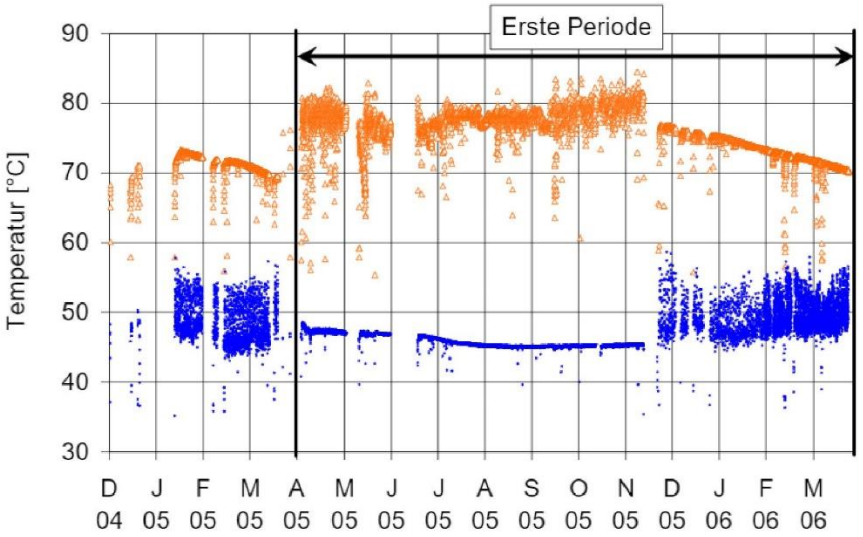

Figure 16: Wellhead temperature (Kabus et al., 2006)

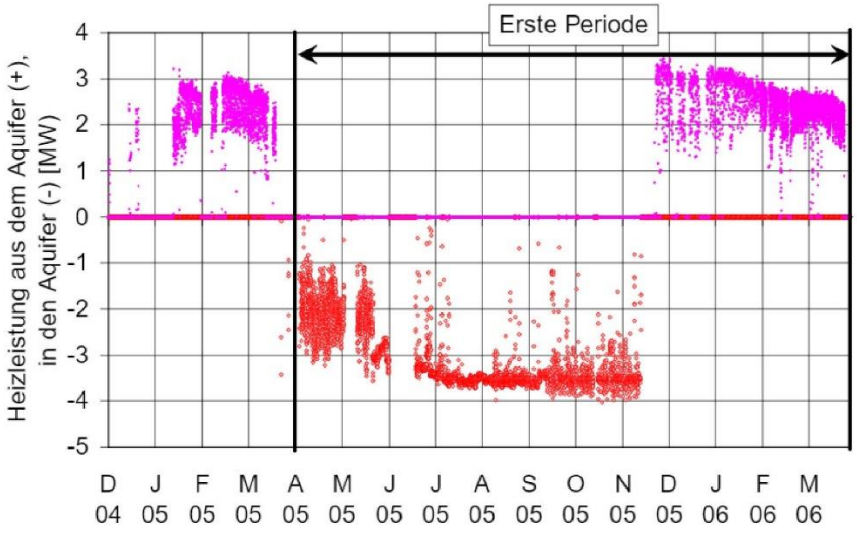

Figure 17: Heating power (Kabus et al., 2006)

The performance of the storage in principle was good but was eventually shut down in 2019. The reason was the lack of heating demand and therefore the shift to a surface storage utility with a shorter reaction time. The only operational problem occurring was the failure of a pump due to corrosion in 2008 (Fleuchaus, 2020, p.70).

The overall efficiency of the ATES between 2005 and 2014 was 56% because of the lack of an adequate heat source. When the injection pump in 2008 failed injection was not possible and thus two production circles were performed thus delivering a return rate of 78% (Schäfer, 2016). The HEATSORE project systematically analyses past experience with previous ATES projects mainly in the Netherlands. Practical experience concerning completion and production, simulation methods, operational efficiency, and cost efficiency was collected and analyzed. Possible problems, and problems encountered were also analyzed.

This all, with the goal of customizing high to medium temperature ATES that help meet heat demand in winter utilizing renewable energy mostly generated in summer by storing it. Of course, at best excess energy because its cheap and otherwise would be wasted.

9 Conclusion

Every business opportunity that builds on the idea of being supplied by heating power from a borehole must fulfill two requirements. Firstly, it must have a heating demand which also means a certain temperature has to be maintained. Secondly the temperature level maintained in the business opportunity must be low enough to allow power supply from the borehole.

Business opportunities that have good chances to fulfill those criteria were researched and the best options investigated closer. Growing plants in greenhouses, growing sea creatures in aquacultures, and producing methane in biogas production facilities were the applications chosen for investigation.

Assessing the business opportunities requires a clear understanding about the capabilities of the well to provide geothermal power and knowledge about the power demand the individual applications require. Both was done within this thesis. The capabilities of the well was assessed by simulating a borehole heat exchanger. It was the system chosen to be used for heat extraction from the borehole because of easy realization and operations. Simulations were not limited to only address certain applications but cover a broad range of different conductivities, flowrates, depth, inflow, and outflow temperatures. By doing so the results can now be used to evaluate all kinds of applications. The power demand for different applications was extracted from different publications during the literature research and in one case data were supplied direct from the investigated business opportunity. After addressing heating demand and supply a clear performance measure was calculated. For aquaculture and greenhouses this performance measure was translated to square meters of production possibility. For biogas it is the volume of methane that can be produced per year. The performance measure provides a very good impression on the size in which business opportunities come depending on the well depth and the conductivity of the surrounding formation. Greenhouses were after a financial assessment deemed not to be a viable business. Biogas facilities show some promising results for wells deeper than 2000m. Aquacultures show the most potential and should undergo further investigation.

Another idea is to not only use the well but also the adjacent reservoir for extending oil and gas well life. This can be realized by creating an aquifer thermal energy storage. A concept that has proven its applicability from 2005 to 2019 in Neubrandenburg.

Future studies should address requirements in terms of size for the business opportunities to be profitable. Also, a more thorough assessment of the heat demand could prove to be useful since it would give insight on possible measures for increasing the energy efficiency of business applications. Investigations on how to bring additional energy to the applications for example by using solar energy could proof to be beneficial.

10 References

[1] **Baeza, E. J., Dijkxhoorn, Y., Logatcheva, K., Hennen, W., Splinter, G., Stanghellini, C. and Hemming, S.** (2021) *Business case for large scale crop production in greenhouse facilities in Iceland for the global market,* WUR GTB Tuinbouw Technologie.

[2] **Bakima, G., Pittens, B., Buikn Nick and Drijver, B.** (2019) *HEATSTORE Design Considerations for high temperature storage in Dutch aquifers* HEATSTORE-D1.1, Appendix II [Online]. https://www.heatstore.eu/downloads.html

[3] **Baudion, W., Nono-Womdim, R., Lutaladio, N. and Hodder, A**. (eds) (2013) *Good agricultural practices for greenhouse vegetable crops: Principles for Mediterranean climate areas* (Food and Agriculture Organization of the United Nations Plant Production and Protection Division), Rome, Food and Agricultural Organization of the United Nations (FAO).

[4] **Baudoin, W., Nersisyan, A., Shamilov, A. and Gutierrez, D**. (eds) (2017) *Good Agricultural Practices for greenhouse vegetable production in the South East European countries: Principles for sustainable intensification of smallholder farms*, Rome.

[5] **Cengel, Y.** (2011) *Heat Transfer; A Practical Approach*, 2nd edn, McGraw-Hill Professional.

[6] **Engindeniz, S. and Tuzel, Y.** (2006) 'Economic analysis of organic greenhouse lettuce production in Turkey', *Scientia Agricola*, vol. 63, no. 3, pp. 285–290.

[7] **Fazeli, F.** (2020) 'Subsurface Production System Design, Flow Assurance and Artificial Lift'.

[8] **Fernández, M. D., Gallardo, M., Bonachela, S., Orgaz, F., Thompson, R. B. and Fereres, E.** (2005) 'Water use and production of a greenhouse pepper crop under optimum and limited water supply', *The Journal of Horticultural Science and Biotechnology*, vol. 80, no. 1, pp. 87–96.

[9] **Fleuchaus, P.** (2020) *Global application, performance and risk analysis of Aquifer Thermal Energy Storage (ATES)*, Dissertation, Karlsruhe, Karlsruher Instituts für Technologie.

[12] **Fleuchaus, P., Godschalk, B., Stober, I. and Blum, P.** (2018) 'Worldwide application of aquifer thermal energy storage – A review', *Renewable and Sustainable Energy Reviews*, vol. 94, pp. 861–876.

[11] **Fruhwirth, R.** (2020/21) 'Energy Efficiency in Petroleum production part II', p. 115.

[12] **Fruhwirth, R. K. and Hofstätter, H.** (2016) 'An innovative approach for optimising geothermal energy recovery / Tiefe geothermische Energiegewinnung - Innovative Wege zur Optimierung', *Geomechanics and Tunnelling*, vol. 9, no. 5, pp. 489–496.

[13] **Hangartner, D., Hellweg, S., Stössl, F. and Juraske, R.** (2010) *Model for heating demand in greenhouses,* Energy Science and Technology ETHZ.

[14] **Hatirli, S. A., Ozkan, B. and Fert, C.** (2006) 'Energy inputs and crop yield relationship in greenhouse tomato production', *Renewable Energy*, vol. 31, no. 4, pp. 427–438.

[15] **Hepbasli, A.** (2011) 'A comparative investigation of various greenhouse heating options using exergy analysis method', *Applied Energy*, vol. 88, no. 12, pp. 4411–4423.

[16] **Kabus, F., Hoffmann, F. and Möllmann, G.** (eds) (2005) *Aquifer Storage of Waste Heat Arising from a Gas and Steam Cogeneration Plant - Concept and First Operating Experience* [Online] www.geothermal-energy.org/pdf/IGAstandard/WGC/2005/1505.pdf.

[17] **Kabus, F., Richlak, U. and Beuster, H.** (2006) *Neubrandenburg Saisonale speichernung von Überschusswärme aus einem Heizkraftwerk in einen Aquifer in Neubrandenburg,* GNT Geothermie Neubrandenburg GmbH [Online]. Available at https://docplayer.org/15338809-Saisonale-speicherung-von-ueberschusswaerme-aus-einem-heizkraftwerk-in-einen-aquifer-in-neubrandenburg.html.

[18] **Kleine Mölle, P. and Dürr, C.** (2016) *Ökonomische und ökologische Betrachtungen zur Erhöhung der Methanausbeute von Biogasanlagen,* ESB Business School, Hochschule Reutlingen [Online]. https://publikationen.uni-tuebingen.de/xmlui/handle/10900/72350

[19] **Klinghoffer, N. B. and Castaldi, M. J.** (eds) (2013) *Waste to energy conversion technology*, Oxford UK, Woodhead Publishing Limited.

[20] **Langbauer, C.** (2020) 'Surface Facilities for Geothermal Energy', p. 12.

[21] **Lorenz, J., Yung, D., Panchal, C. and Layton, G.** (1982) *Assessment of heat-tranfer correlations for turbulent water flow through a pipe at Prandtl numbers of 6. 0 and 11. 6*.

[22] **Mohammadi, A. and Omid, M.** (2010) 'Economical analysis and relation between energy inputs and yield of greenhouse cucumber production in Iran', *Applied Energy*, vol. 87, no. 1, pp. 191–196.

[23] **Rafferty, K.** (1991) 'Geothermal direct use Engineering and design Guidbook'.

[24] **Schäfer, A.** (2016) *Geothermische Nutzung des tiefen Untergrundes in Neubrandenburg: Aquiferwärmespeicher vermittelt zwischen GuD-Kraftwerk und Fernwärmenet* [Online], Neubrandenburg. Available at http://docplayer.org/62168769-Geothermische-nutzung-des-tiefen-untergrundes-in-neubrandenburg-aquiferwaermespeicher-vermittelt-zwischen-gud-kraftwerk-und-fernwaermenetz.html.

[25] **Śliwa, T., Kruszewski, M., Sapińska-Śliwa, A. and Assadi, M.** (2017) 'The application of Vacuum Insulated Tubing in Deep Borehole Heat Exchangers', *AGH Drilling, Oil, Gas*, vol. 34, no. 2, p. 597.

[26] T**abatabaei, M. and Ghanavati, H.** (2018) *Biogas*, Cham, Springer International Publishing.The 12th International Conference on Energy Storage (ed) (2012) *High-temperature aquifer thermal energy storage (HT-ATES): sustainable and multi-usable* [Online], Innostock. Available at chrome-extension://efaidnbmnnnibpcajpcglclefindmkaj/viewer.html?pdfurl=https%3A%2F%2Fwww.iftechnology.com%2Fwp-content%2Fuploads%2F2018%2F05%2FDrijver-et-al-2012-High-temperature-aquifer-thermal-energy-storage-HT-ATES-sustainable-and-multi-usable-1.pdf&clen=507070&chunk=true.

[27] **Toth, A.** (2016) *Flow and Heat Transfer in Geothermal Systems: Basic Equations for Describing and Modelling Geothermal Phenomena and Technologies* [Online], Saint Louis, Elsevier Science. Available at http://gbv.eblib.com/patron/FullRecord.aspx?p=4717201.

[28] **Utinger, A., Arthur Wellinger, Trachsel Daniel and Scharfy Deborah** (2019) *Leitfaden-Abwaermenutzung_auf_Biogasanlagen* [Online]. Available at https://pubdb.bfe.admin.ch/de/publication/download/9745.

[29] **Vetter, A., Mangelsdorf, K., Schettler, G., Seibt, A., Wolfgramm, M., Rauppach, K. and Vieth-Hillebrand, A.** (2012) 'Fluid chemistry and impact of different operating modes on microbial community at Neubrandenburg heat storage (Northeast German Basin)', *Organic Geochemistry*, vol. 53, pp. 8–15.

[30] **Willhite, G. P.** (1967) 'Over-all Heat Transfer Coefficients in Steam and Hot Water Injection Wells'.

[31] **Wolfgramm, M. and Seibt, A.** (2006) *Neubrandenburg Geochemisches Monitoring des geothermalen Tiefenspeichers in Neubrandenburg* [Online]. Available at http://docplayer.org/43816798-Geochemisches-monitoring-des-geothermalen-tiefenspeichers-in-neubrandenburg-markus-wolfgramm-andrea-seibt.html.

[32] **Zenke, J., Seibt, P. and Kabus, F.** (2000) 'Increase of the efficiency of the Neubrandenburg geothermal heating Plant through surplus heat storage in Summer'.

List of Tables

List of Figures

Abbreviations

ATES	Aquifer thermal Energy Storage
BHE	Borehole Heat Exchanger
FR	Flowrate
EGS	Enhanced Geothermal System
GHP	Geothermal Heating Plant

Appendix A

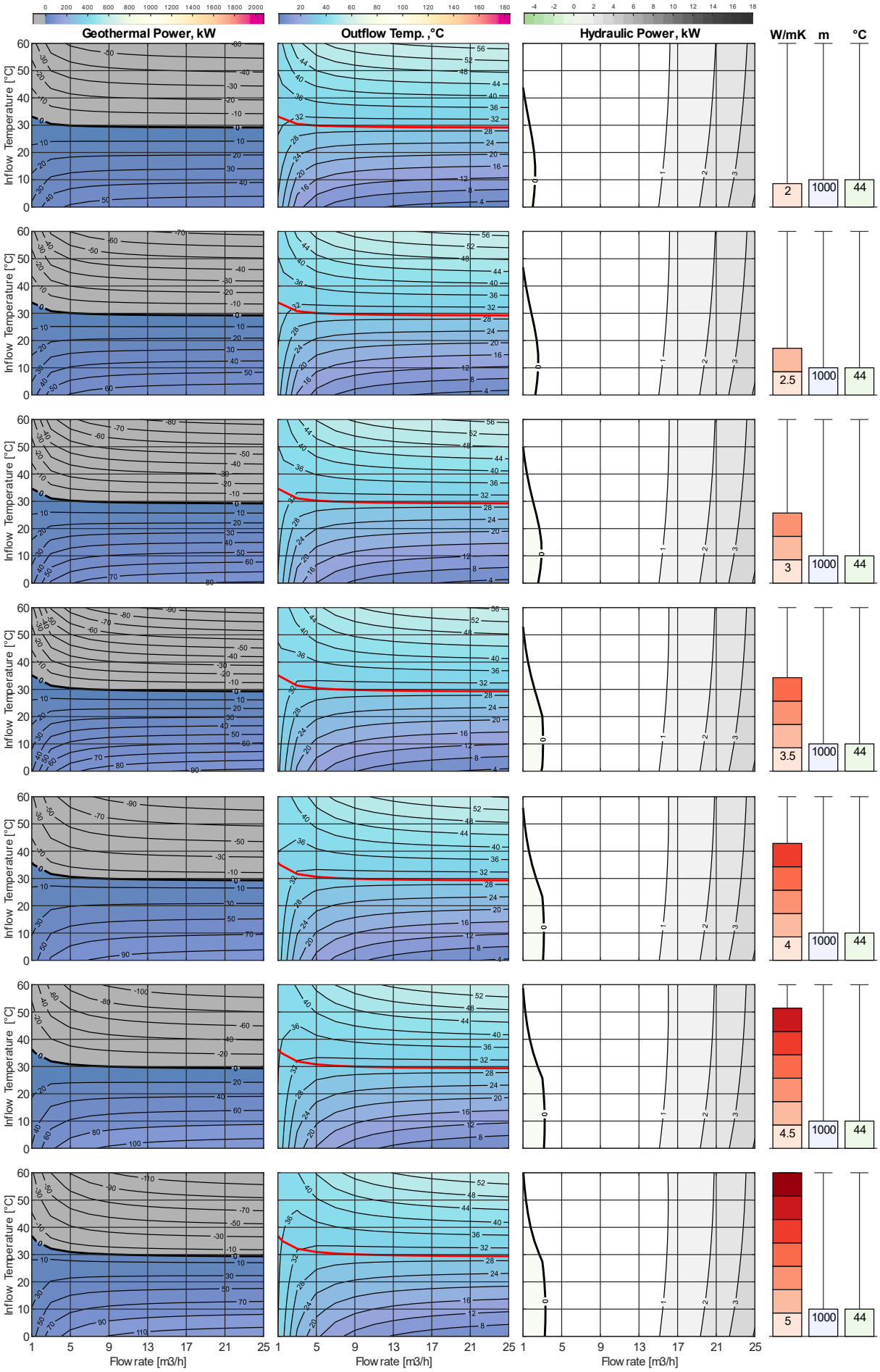
Geothermal Power, kW
Outflow Temp. ,°C
Hydraulic Power, kW
W/mK
m
°C
Inflow Temperature [°C]
Flow rate [m3/h]
2
1000
44
2.5
1000
44
3
1000
44
3.5
1000
44
4
1000
44
4.5
1000
44
5
1000
44

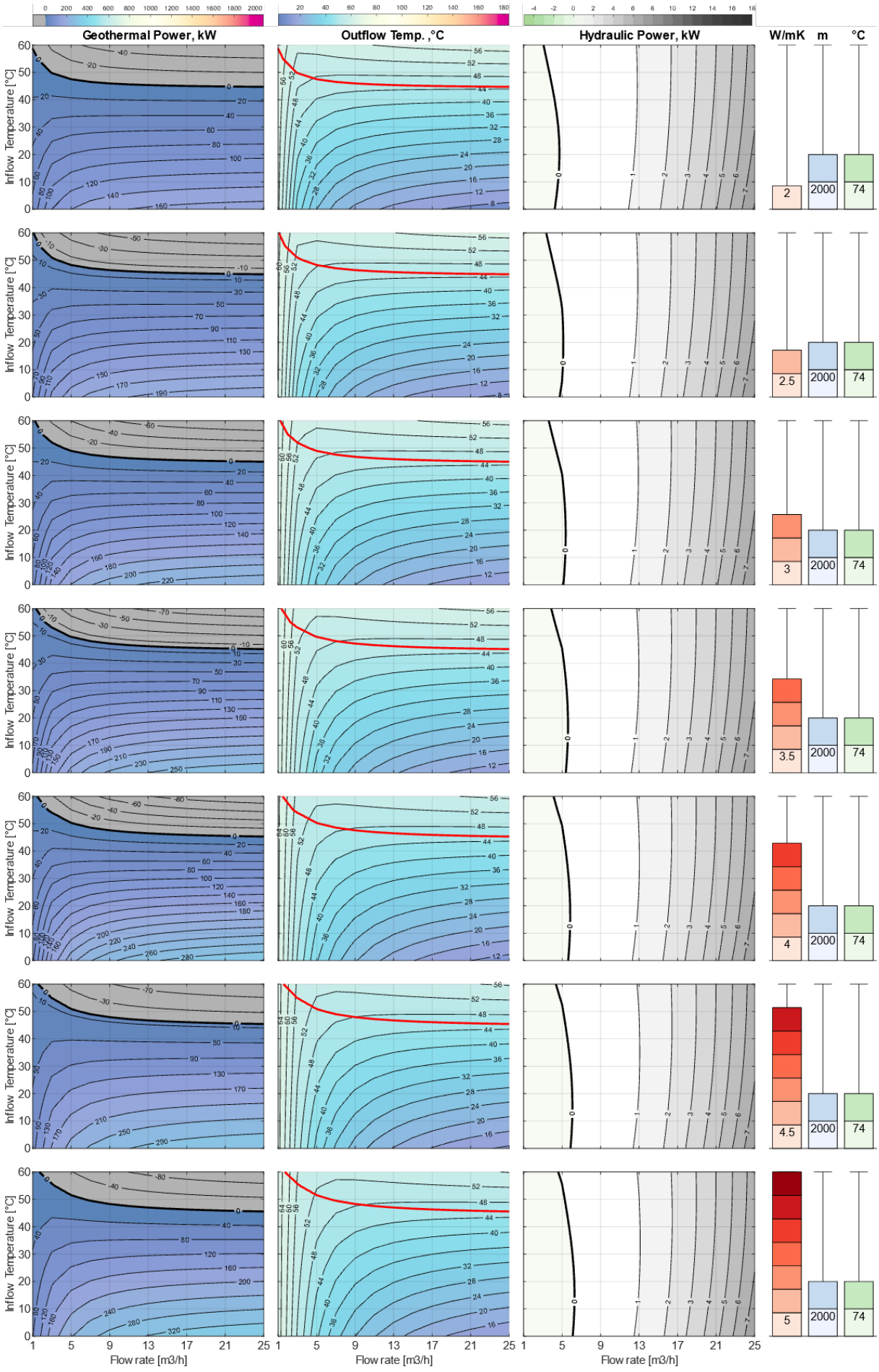
Geothermal Power, kW
Outflow Temp. ,°C
Hydraulic Power, kW
W/mK
m
°C
Inflow Temperature [°C]
Flow rate [m3/h]
2
2000
74
2.5
2000
74
3
2000
74
3.5
2000
74
4
2000
74
4.5
2000
74
5
2000
74

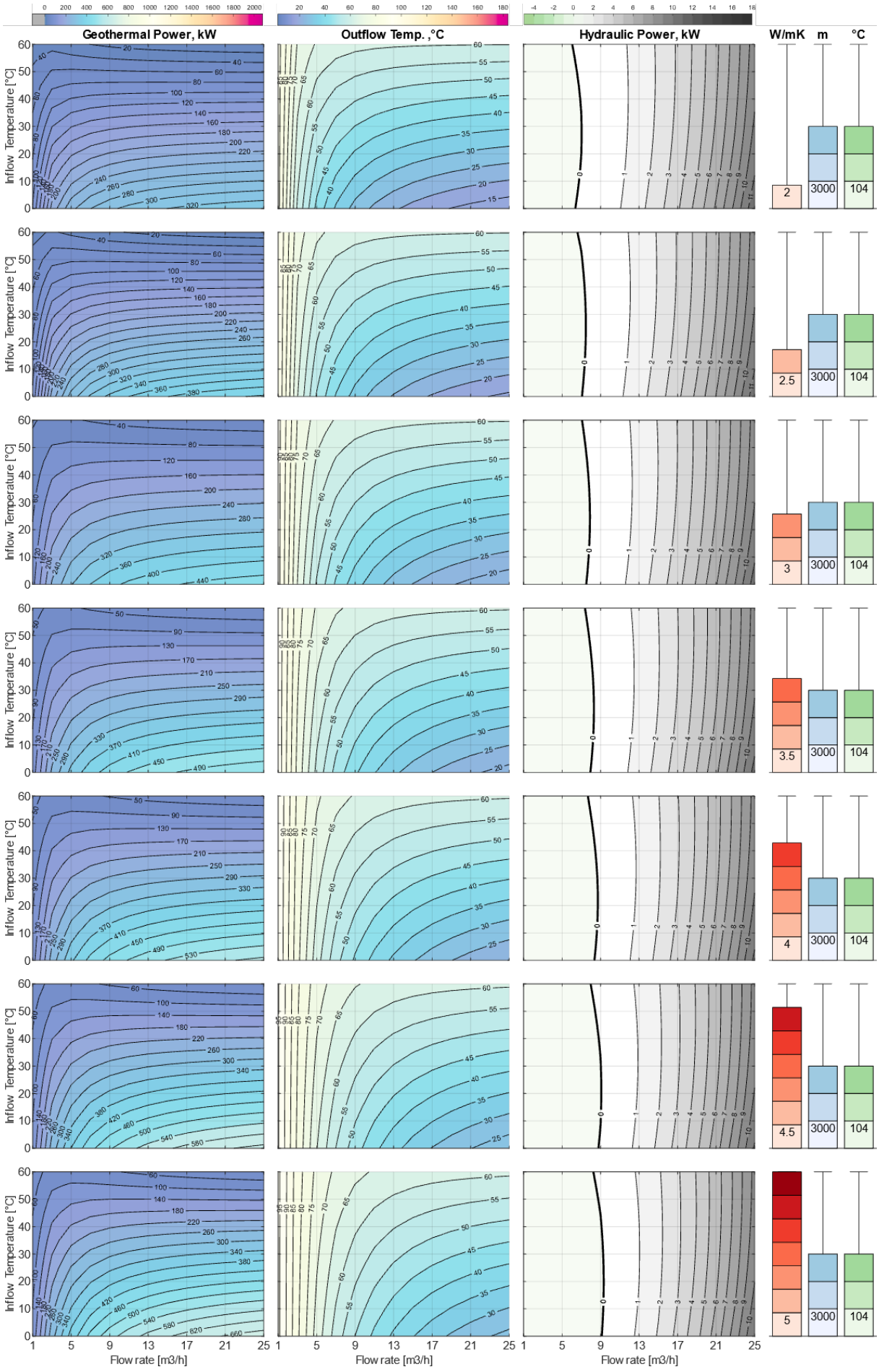
Geothermal Power, kW
Outflow Temp. ,°C
Hydraulic Power, kW
W/mK
m
°C
Inflow Temperature [°C]
Flow rate [m3/h]
2
3000
104
2.5
3000
104
3
3000
104
3.5
3000
104
4
3000
104
4.5
3000
104
5
3000
104

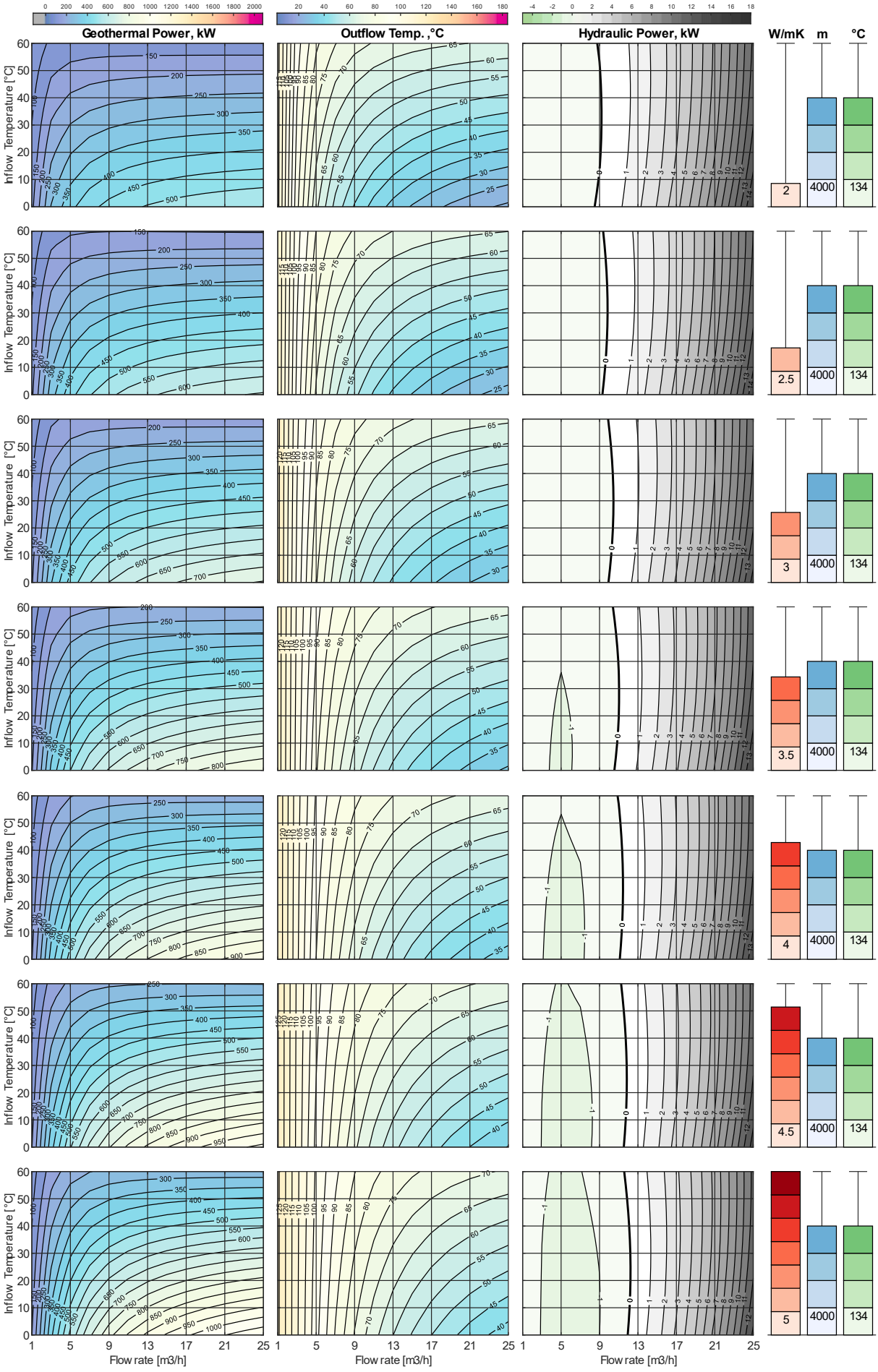
Geothermal Power, kW
Outflow Temp. ,°C
Hydraulic Power, kW
W/mK
m
°C
Inflow Temperature [°C]
Flow rate [m3/h]
2
4000
134
2.5
4000
134
3
4000
134
3.5
4000
134
4
4000
134
4.5
4000
134
5
4000
134

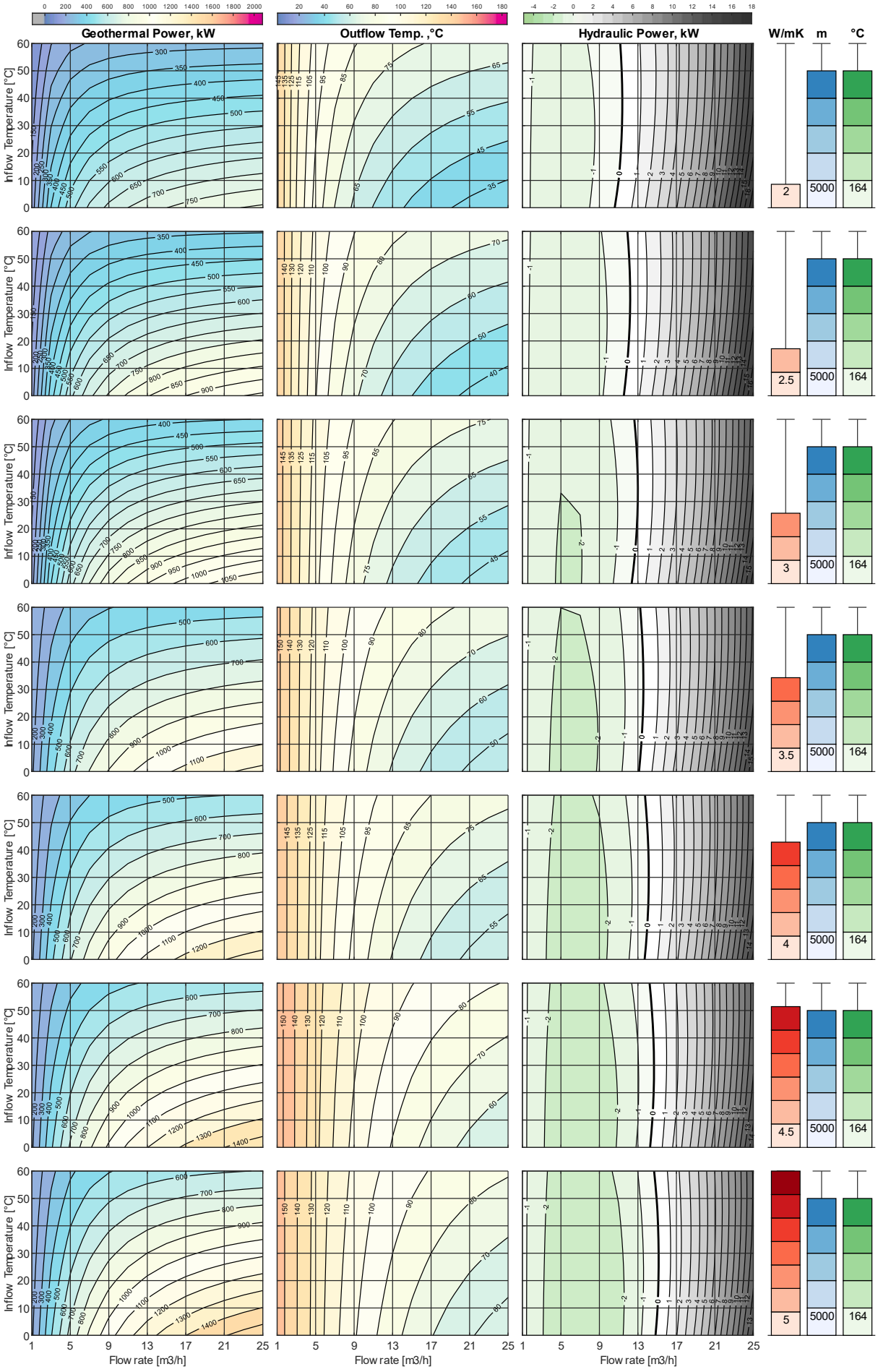
Geothermal Power, kW
Outflow Temp. ,°C
Hydraulic Power, kW
W/mK
m
°C
Inflow Temperature [°C]
Flow rate [m3/h]
2
2.5
3
3.5
4
4.5
5
5000
164

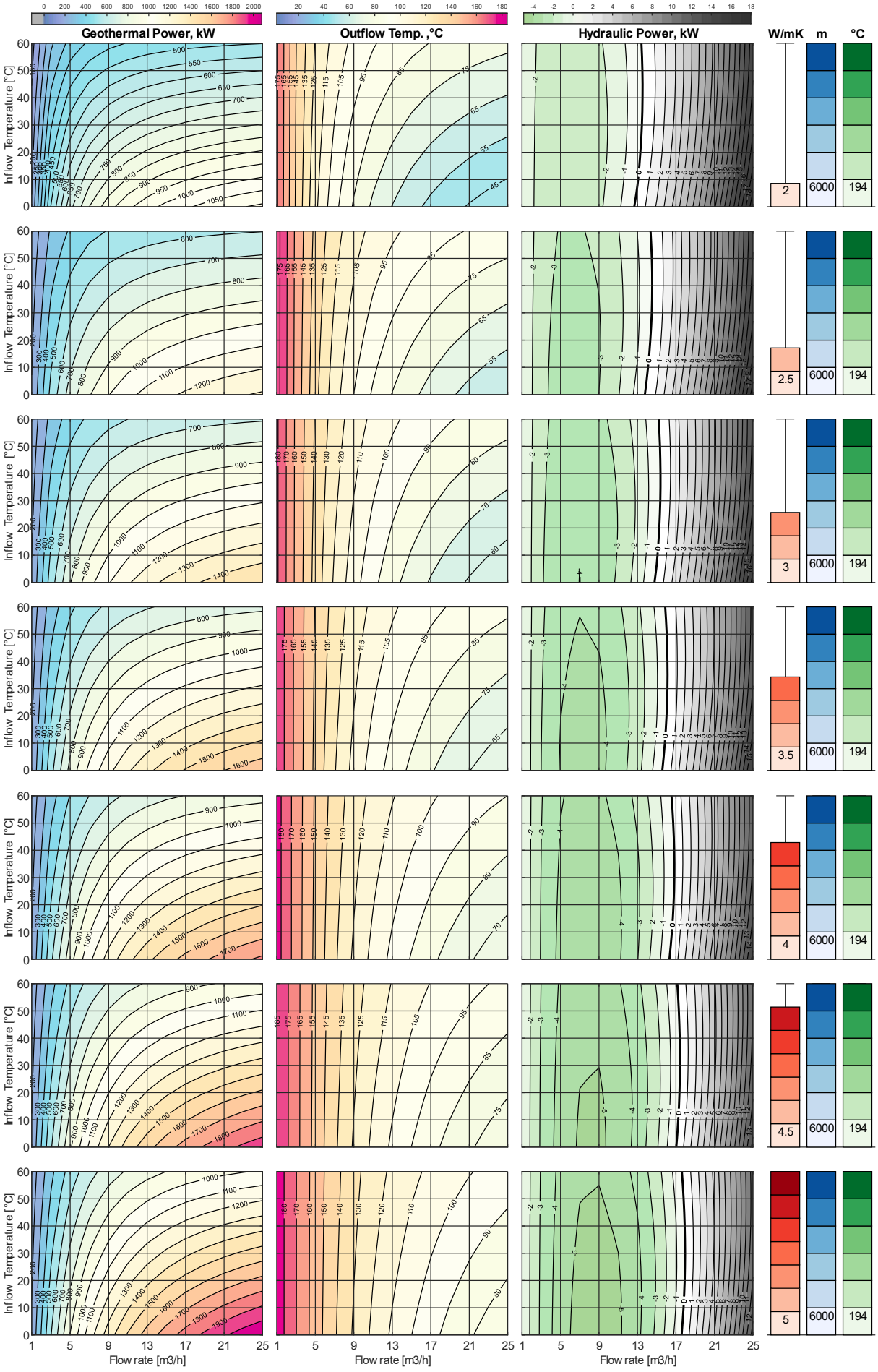
Geothermal Power, kW
Outflow Temp. ,°C
Hydraulic Power, kW
W/mK
m
°C
Inflow Temperature [°C]
Flow rate [m3/h]
2
2.5
3
3.5
4
4.5
5
6000
194